Monte Carlo eikonal scattering

W. R. Gibbs[1] and J. P. Dedonder[2]
[1]*New Mexico State University, Las Cruces, New Mexico 88003, USA*
[2]*Laboratoire de Physique Nucléaire et Hautes Énergies, Universités Pierre et Marie Curie et Paris-Diderot, IN2P3 et CNRS 4, place Jussieu, 75252 Paris cedex 05, France*
(Received 1 March 2012; published 16 August 2012)

Background: The eikonal approximation is commonly used to calculate heavy-ion elastic scattering. However, the full evaluation has only been done (without the use of Monte Carlo techniques or additional approximations) for α-α scattering.
Purpose: Develop, improve, and test the Monte Carlo eikonal method for elastic scattering over a wide range of nuclei, energies, and angles.
Method: Monte Carlo evaluation is used to calculate heavy-ion elastic scattering for heavy nuclei including the center-of-mass correction introduced in this paper and the Coulomb interaction in terms of a partial-wave expansion. A technique for the efficient expansion of the Glauber amplitude in partial waves is developed.
Results: Angular distributions are presented for a number of nuclear pairs over a wide energy range using nucleon-nucleon scattering parameters taken from phase-shift analyses and densities from independent sources. We present the first calculations of the Glauber amplitude, without further approximation, and with realistic densities for nuclei heavier than helium. These densities respect the center-of-mass constraints. The Coulomb interaction is included in these calculations.
Conclusion: The center-of-mass and Coulomb corrections are essential. Angular distributions can be predicted only up to certain critical angles which vary with the nuclear pairs and the energy, but we point out that all critical angles correspond to a momentum transfer near 1 fm^{-1}.

DOI: 10.1103/PhysRevC.86.024604 PACS number(s): 25.70.Bc, 25.55.Ci, 24.10.Lx

I. INTRODUCTION

Monte Carlo (MC) methods are very valuable for performing multidimensional integrals, especially in quantum applications [1]. Recently, MC calculations of nuclear structure have been performed, both for light nuclei [2,3] and with the nuclear shell model [4]. In the present article we study the use of this technique for the evaluation of multidimensional integrals in the calculation of elastic scattering of heavy ions in the eikonal approximation.

Monte Carlo techniques have been used for classical simulations of nuclear reactions for many years (see, e.g., Ref. [5] and references within). In that case (highly inelastic reactions), the assumption that phase information is unimportant appears to be valid, at least under certain conditions. This technique can reveal properties of nuclear reactions for inelastic reactions where many channels are open. Much less use has been made of the MC method for elastic (or nearly elastic) reactions. The reason for this might be that integrals performed with Monte Carlo methods are deemed not to be suitable for producing the highly oscillating amplitudes because of the growth in errors that typically occurs in this case. As we shall see shortly the evaluation of the Glauber elastic scattering amplitude does not suffer from this problem. We now review some of the literature on this problem.

A. Review

1. The use of the Glauber approximation for nucleus-nucleus scattering

Before discussing the use of Monte Carlo methods for eikonal calculations, we briefly mention the applications of the Glauber scattering method to heavy-ion scattering more generally.

Franco and Yin [6] and Yin *et al.* [7] were the first to evaluate the full sum for the α-α scattering amplitude which appears to be the largest case for which the full scattering amplitude can be evaluated without further approximation and without the use of Monte Carlo methods. Their method relies on the use of a Gaussian approximation for the nuclear density. Abu-Ibrahim *et al.* [8] evaluated the full Glauber multiple-scattering amplitude for proton-^{6}He scattering.

Al-Khalili, Thompson, and Tostevin [9] studied the ^{11}Li halo structure using eikonal methods, Al-Khalili and Tostevin [10] studied the relation of reaction cross section to radii in the Glauber model, They also studied proton helium halo nuclei [11] with Glauber scattering and in Ref. [12], with Brooke, they treated ^{11}B + ^{12}C scattering with non-eikonal corrections, modifying the trajectory at lower energies. El-Gogary [13] treated cluster nuclei to evaluate the Glauber formula. El-Gogary *et al.* [14] used an approximate center-of-mass correction with a double-Gaussian form for the density. Franco and Varma [15] treated the center-of-mass effects to several orders and compared their results (primarily) with total cross sections. El-Gogary *et al.* [16] did calculations with an approximate center-of-mass correction and noted that a simplified treatment of center-of-mass effects is problematic. Horiuchi *et al.* [17] did a systematic study of reaction cross sections using an improved expansion of the Glauber formula. Zhong [18] calculated nucleus-nucleus scattering in an α-cluster model with double-Gaussian forms for the density. Charagi and Gupta [19] calculated ^{16}O scattering from several nuclei using the optical limit approximation

(OLA). Abu-Ibrahim and Suzuki [20] used the OLA and a phenomenological profile function to treat a large number of nuclei. Abu-Ibraham *et al*. [21] calculated halo nuclei scattering in the Glauber model. Abu-Ibrahim and Suzuki [22] calculated nucleus-nucleus scattering at intermediate energies using corrections to the OLA. Abu-Ibraham and Suzuki [23] studied the profile function in heavy-ion scattering. Franco and Nutt [24] treated short-range correlations in heavy-ion scattering. Lenzi *et al*. [25,26] did a systematic study of heavy-ion scattering in an OLA treatment of eikonal scattering.

2. Monte Carlo method

The Monte Carlo method has been used to evaluate the eikonal amplitude on several occasions.

Zadorozhny, Uzhinsky, and Shmakov [27] were perhaps the first to apply the eikonal Monte Carlo method but no details are given. Merino, Novikov, and Shabelski [28] very recently compared methods for radius extraction. One of the methods is exact with Monte Carlo using the Metropolis algorithm [29]. Alkhazov and Lobodenko [30] calculated reaction cross sections for halo nuclei using the Monte Carlo method. Shmakov, Uzhinskii, and Zadorozhny [31] used Monte Carlo techniques for the generation of inelastic diagrams. Krpic and Shabelski [32] used the Metropolis algorithm to calculate elastic and inelastic scattering from several nuclei using a diagrammatic expansion. They neglected the center-of-mass correction. Abu-Ibrahim and Suzuki [33] studied low-energy ^{6}He-^{12}C scattering using the optical eikonal potential evaluated with a Monte Carlo technique.

Recently, Varga *et al*. [34] have combined the Monte Carlo Green's function method of solution of few-body problems with Glauber theory to calculate α-α and halo-nuclei scattering with no approximation beyond those inherent in basic eikonal theory. No doubt this method should be used in any case in which an exact calculation of the nuclear structure is available but a much more common case is the scattering of heavier nuclei where such a solution is still for the future. In this case less ambitious approximations to the nuclear densities need to be used. We later will show calculations comparing the two methods and it would seem that the details (short-range correlations) make little difference.

3. Center-of-mass correction

Of the above methods only that of Varga *et al*. [34] includes the center-of-mass correction exactly. We will see that this correction is very important, even for heavier nuclei.

Chauhan and Khan [35] treated ^{12}C-^{12}C elastic scattering and found that center-of-mass effects play an important role. They use an expansion of the profile function. Liu *et al*. [36] calculated α scattering from several nuclei at 1.37 GeV. They used an overall factor for the center-of-mass correction and varied the phase of the nucleon-nucleon interaction.

Franco and Tekou [37] calculated the optical model version up to fifth order. They included corrections for the center of mass. Shukla [38] included the center-of-mass and Coulomb effects to investigate reaction cross sections.

4. Coulomb correction

The basic Glauber method does not include the Coulomb interaction, and a correction (often very important) must be made for it after the calculation.

Londratyuk and Kopeliovich [39] argued that it would be a good approximation to simply add the strong and Coulomb phases. Glauber and Matthiae [40] and Czyz, Lesniak, and Wolek [41] used mainly this approximation. The corrections to this approximation were developed using various techniques but most often were based on an optical potential. See Ref. [42] for a recent treatment and references to the previous work for the application to pion-nucleon scattering. Fäldt and Pilkuhn [43] used a semiclassical method with the Glauber model to correct for the Coulomb modification of the trajectories. This technique has the advantage that an optical model fit does not have to be made to the data to find the correction factors. While they developed the method for pion-nucleus scattering it is currently being applied to heavy-ion elastic scattering. These two methods will be treated shortly is some detail. Charagi and Gupta [44] treated low-energy heavy-ion scattering in the Coulomb-modified optical limit in two papers. Cha [45] introduced the deviation of the orbit in the Glauber model from the nuclear potential as well as the Coulomb potential. Charagi [46] commented on the Coulomb correction to the Glauber model introduced by Cha [45], saying that it failed to reproduce known reaction cross sections. Alvi *et al*. [47] calculated α-nucleus scattering treating the system by phenomenology (fitting to Ni) and showed the Coulomb effect. Ahmad *et al*. [48] calculated ^{12}C-^{12}C elastic scattering using the first two terms of an expansion in a Coulomb-modified Glauber calculation.

B. Organization

The paper is organized as follows. In Sec. II we describe the method, showing how to satisfy the center-of-mass condition with Monte Carlo sampling. In particular, the technique for determining an auxiliary density which results in a desired center-of-mass single-particle density is developed. In this section the method for making the Coulomb correction is also presented.

In Sec. III the calculations are compared with data for 20 nuclear pairs and energies. The parameters for the auxiliary functions are given.

In Sec. IV the results are summarized and conclusions are drawn.

In the the appendices we present a method for the rapid partial-wave projection of the Glauber amplitude and explain how the variation calculation for the ^{4}He density was done.

II. MONTE CARLO EIKONAL NUCLEUS-NUCLEUS SCATTERING

A. The Glauber method

The eikonal theory of elastic scattering as expressed by Glauber [49] and elaborated and studied by others [50–54] is believed to be an accurate representation of scattering

at high energies and forward angles. It can be applied to calculate multiple scattering of a simple projectile on a nucleus or collisions between nuclei, taking into account all of the scatterings possible in this theory.

There are two major difficulties in applying this technique: (1) as the atomic number of the scatterers increases the number of scatterings becomes very large and (2) the representation of the wave function (density) of the two scattering conglomerates raises the problem of the center of mass. The use of Monte Carlo techniques is well suited to solve both of these problems.

For the scattering of α particles on ^{4}He (the largest case treated to date for the full scattering series without using Monte Carlo methods) there are 16 possible scatterings. By taking into account all of the possible orders there are $2^{16} - 1 = 65\,535$ terms in the multiple-scattering expansion. They are not all independent however and, by dividing them into classes, the calculation can be reduced [7] to 37 different types, each characterized by a 4×4 matrix of zeros and ones to be calculated and included with different weights. There remains a 24-dimensional integral to be done for each term. By using a Gaussian representation of the wave function of ^{4}He, Franco and Yin [6] and Yin *et al*. [7] were able to provide expressions for these integrals and calculate the full sum.

In the present paper the Glauber expression for multiple scattering is used directly as a product of factors without expanding them into separate terms and the integral over the many-body nuclear density is done with Monte Carlo techniques, either with direct sampling or with the Metropolis algorithm. Normally, one would be reluctant to use a Monte Carlo method to obtain a rapidly oscillating function as the amplitude for scattering, but in this case a Monte Carlo method can be used to calculate the profile function (which is a smooth function since it consists of a sum of analytic functions) and then a standard numerical technique can be applied to perform the last (one-dimensional) integral. The explicit development of the method is given in Sec. II B.

The exact wave function for a nucleus at rest as a function of the coordinates of the nucleons (if we ignore spin for the present) would necessarily be translationally invariant in the absence of external interaction. In order to calculate the scattering between the two nuclei one would simply translate the wave function to place the center of mass at the origin. Of course, one rarely has the exact wave function available but it is possible to introduce an approximate density which is, indeed, translationally invariant where one can carry out this procedure. For ^{4}He the four-body problem can be solved using Monte Carlo methods [2,3]. In the first instance a variational wave function can be used to find the minimum in energy by varying the parameters in the trial function. The trial wave function should be translationally invariant. The square of the wave function (the density, which is all that is needed for the Glauber scattering calculation) is represented by a collection of Metropolis walkers.

What has more commonly been done in practice is to start with an approximation to the density, which is obtained empirically from a probe which is sensitive to the single-particle density relative to the center of mass, most often electron scattering. One then applies some transformation to ensure that the center of mass of the nucleus is at the origin. Franco and Yin [6] gave a prescription and showed that, using this formula, one could calculate with the fixed-well assumption (for a harmonic oscillator potential) and then apply an exact correction. To illustrate the importance of this correction we point out that the factor by which the amplitude is multiplied for α-α scattering at $-t = 3$ (GeV/c)^2 is 3.6×10^7. Clearly, a careful treatment of the center-of-mass correlation is important. This problem is discussed at length in Sec. II E and the MC method is applied to the evaluation of the Glauber amplitude for α-α scattering in Sec. III A.

It is important to define what one means by a measure of the center-of-mass correction; that is, we need to define the "zero effect" condition. It is common in both the double-folding model and the OLA to take the density from electron scattering (corrected for the charge distribution of the proton) to form a product density. Often the center-of-mass requirement is ignored in these calculations (see however Franco and Varma [15] for a first-order treatment). We will take this product density as our "no effect" model and compare the scattering from this case with scattering from a density with the proper center-of-mass properties. We will see that ignoring the center-of-mass effect, even for fairly heavy nuclei, is ill advised.

B. Basic technique

The expressions for the Glauber amplitude are available many places; see, e.g., Franco and Yin [6].

The nuclear profile function, $G(\mathbf{b})$, is the central function in the theory and is given by

$$G(\mathbf{b}) = \int \prod_{i=1}^{A} d\mathbf{s}_i \prod_{j=1}^{B} d\mathbf{s}'_j \phi^2(\{\mathbf{s}\})\psi^2(\{\mathbf{s}'\})G(\mathbf{b}, \{\mathbf{s}\}, \{\mathbf{s}'\}), \quad (1)$$

In Eq. (1) the notation $\{\mathbf{s}\}$ represents the collection of all of the coordinates of the projectile or target, $\phi(\{\mathbf{s}\})$ denotes the projectile ground-state wave function, and $\psi(\{\mathbf{s}\})$ denotes the target ground-state wave function:

$$G(\mathbf{b}, \{\mathbf{s}\}, \{\mathbf{s}'\}) \equiv 1 - \prod_{i=1}^{A}\prod_{j=1}^{B}[1 - \Gamma_{ij}(\mathbf{b} + \mathbf{s}_i - \mathbf{s}_j)]. \quad (2)$$

The functions $G(\mathbf{b}, \{\mathbf{s}\}, \{\mathbf{s}'\})$ and $\Gamma_{ij}(\mathbf{b} + \mathbf{s}_i - \mathbf{s}_j)$ are functions of the two-dimensional vector $\mathbf{b}$ (in the plane perpendicular to the beam direction) and of only the components of the vectors $\{\mathbf{s}\}$ and $\{\mathbf{s}'\}$ perpendicular to the beam. Hence the components of these last vectors could be freely integrated over in the density functions to provide a projected nuclear density for the target and projectile, often called the thickness functions. For cases in which the integrals are being calculated analytically, this is commonly done, leading to a modified integral in only two dimensions for each nucleon in Eq. (1).

For the Monte Carlo method a large number of realizations of the nuclei are created and then the integral in Eq. (1) is evaluated by averaging the function $G(\mathbf{b}, \{\mathbf{s}\}, \{\mathbf{s}'\})$ over this ensemble of nuclei. Since nuclei are inherently three-dimensional objects, the models used to generate this ensemble create three-dimensional distributions. In the remainder of the

paper we discuss techniques for generating such ensembles. To take the projection of the nuclear densities would entail more work, not less, since we do not know how to directly generate ensembles of projected nuclei. Hence we compute what would be the projection integral in the same set of Monte Carlo evaluations as used for the two-dimensional integration.

The scattering amplitude is given by the two-dimensional Fourier transform of $G(\mathbf{b})$. If there is no direction defined for the nuclear wave function (i.e., we consider only nuclei with ground-state spin zero), there is no dependence on the azimuthal angle of scattering, i.e., $G(\mathbf{b}) = G(b)$, and hence the integral over this angle can be done trivially so that the integral of the profile function is only over the magnitude of $\mathbf{b}$,

$$F(\mathbf{q}) = \frac{ik}{2\pi}\int d^2b e^{i\mathbf{q}\cdot\mathbf{b}} G(\mathbf{b}) = ik\int_0^\infty bdbJ_0(qb)G(b). \quad (3)$$

In Eq. (2) $\Gamma_{ij}(\mathbf{b}+\mathbf{s}_i-\mathbf{s}_j)$ denotes the two-dimensional Fourier transform of the elementary nucleon-nucleon amplitude $f(\mathbf{q})$, i.e.,

$$\Gamma_{ij}(\mathbf{b}) = \frac{1}{2\pi ik}\int d^2q e^{-i\mathbf{q}\cdot\mathbf{b}} f_{ij}(\mathbf{q}) = ge^{-b^2/2a},$$
$$g = \sigma(1-i\rho)/(4\pi a), \quad (4)$$

where the nucleon-nucleon amplitude has been approximated by

$$f_{ij}(q) = \frac{ik\sigma(1-i\rho)}{4\pi}e^{-\frac{1}{2}aq^2}, \quad a = a_R + ia_I, \quad (5)$$

where σ is the nucleon-nucleon total cross section and ρ is the ratio of the real to imaginary part of the forward amplitude. For a discussion of the imaginary part of a, a_I see Ref. [55].

We have assumed a Gaussian approximation as a function of momentum transfer for the nucleon-nucleon amplitude. The scattering parameters needed can be extracted from nucleon-nucleon (NN) scattering data [56] and such a set is shown in Fig. 1 as a function of energy (see Refs [57] and [58] for tables of other determinations of these amplitudes). Of course, one might expect that these amplitudes may well be modified in the nuclear medium (see, e.g., Refs. [59–61]) but it may be useful to make calculations with free values to see how large the corrections are likely to be. We take the free values used in the calculations in this paper from the partial-wave parametrization of Arndt *et al*. [56]. A plot of the free values used is shown in Fig. 1. For more details on the representation of the amplitudes, see the following section.

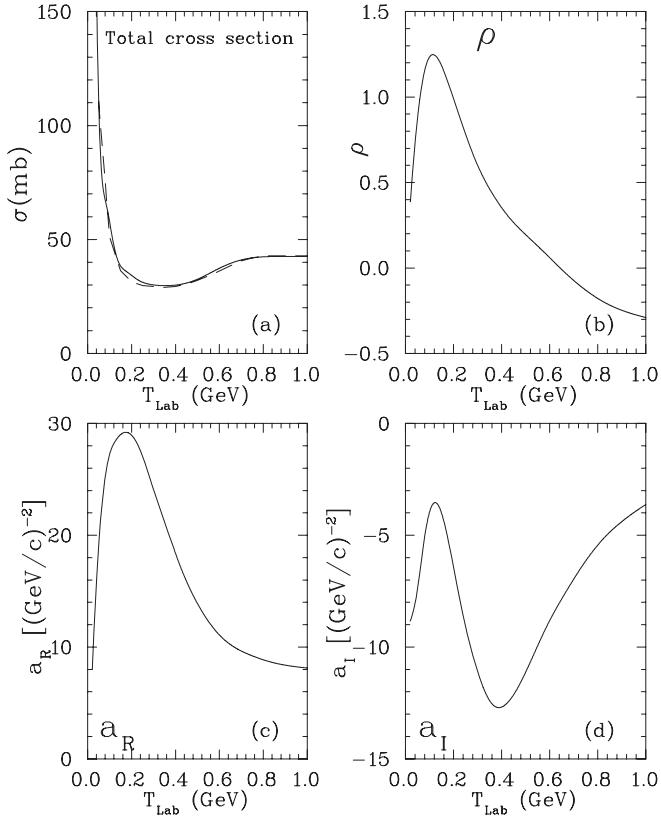

FIG. 1. Nucleon-nucleon parameters taken from the work of Arndt *et al*. [56]. Also shown for the average NN cross section is the recent parametrization of Ref. [61] (dashed line).

C. Nucleon-nucleon amplitude

For NN free-space scattering there are essentially four incoherent beams in the free (and unpolarized) case according to the four possible orientations of the spins of the two colliding nucleons. The imaginary parts of the forward elastic scattering amplitudes give the total cross section for each of these beams. The interference with the Coulomb interaction in the forward direction can give the real parts of these amplitudes averaged with equal weighting.

This combined amplitude is given by

$$A = \tfrac{1}{4}[M_{++++} + M_{----} + M_{+-+-} + M_{-+-+}]$$
$$= \tfrac{1}{2}[M_{++++} + M_{+-+-}] = \tfrac{1}{2}[M_a + M_o], \quad (6)$$

with all amplitudes weighted equally. Here the amplitudes are labeled as "aligned" (subscript "a") and "opposed" (subscript "o"). In the case of nucleus-nucleus scattering the amplitude would still consist of these two amplitudes if spin flip is neglected. Single spin flip amplitudes are very small in the forward direction, so they are often neglected. Since we are considering the scattering of two spin-zero nuclei, a single spin flip is not possible and this small amplitude must enter twice in the calculation so that some other (correlated) nucleon can have its spin flipped in the opposite sense such that the total projection is again zero. These two constraints lead one to consider that the neglect of spin flip is a reasonable approximation.

However, even in the forward direction there is an amplitude M_{+--+} which does not vanish at zero degrees so *a priori* might be expected to contribute. However, we see that this amplitude must flip the spin of one nucleon in each of the nuclei. The resulting spin projection must be reduced to zero again by a second spin flip in each nucleus. This amplitude arises primarily from one-pion exchange. The average over

spin (and isospin) removes this amplitude from consideration, at least in first order, and we neglect it and consider only the amplitude coming from Eq. (6).

The total cross sections which correspond to the two terms in Eq. (6) have been studied experimentally and their difference shows a rapid variation [62] sometimes attributed to a dibaryon (see, e.g., [63]). If some mechanism could be found to change the equal weighting of the aligned and opposite amplitudes in Eq. (6) then a change in the energy dependence of the nucleon parameters could be expected. However, the spin projections come from two different nuclei so it is difficult to see how such a correlation might come about. The amplitude in Eq. (6) does not correspond to any directly measurable differential cross section as a function of angle. Any attempt to extract the parameters directly from a measured differential cross section will lead to parameters not suitable for calculations using the Glauber expressions; the amplitude is a theoretical construct. Each of the terms in Eq. (6) can be well represented in the approximate form of Eq. (5) (see Fig. 2).

Listed in Table I are values of the parameters used in the calculations presented in this paper. Also given are the maximum values of the center-of-mass angle and $-t$.

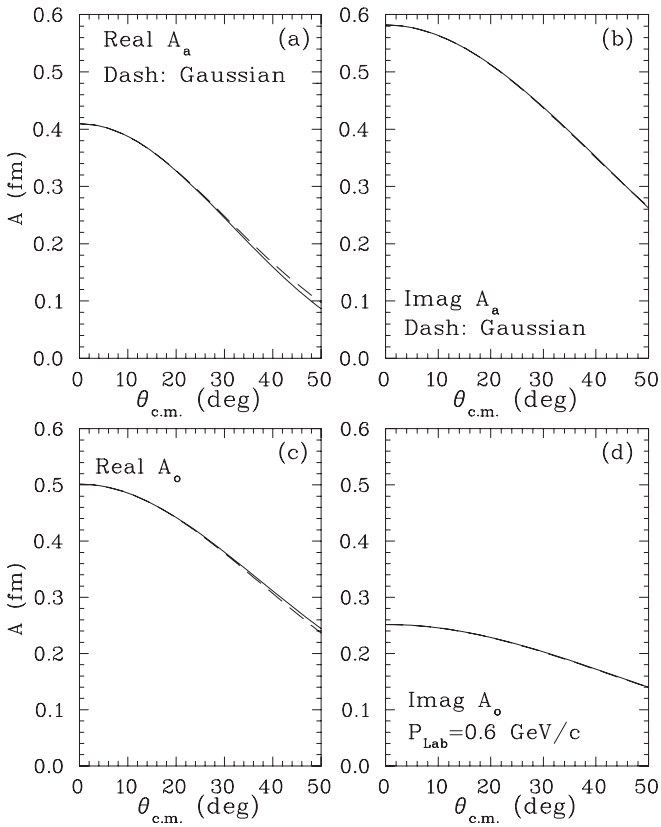

FIG. 2. Angular distribution of the nucleon-nucleon amplitudes taken from the phase-shift analysis of Arndt *et al.* [56]. Also shown is the Gaussian approximation (dashed line) as used in Eq. (5) with parameters chosen to match the value and slope in the forward direction. The "aligned" amplitudes are shown in the upper panels and the "opposite" amplitudes in the lower panels.

D. Nuclear profile function

Another advantage of the method is that the nuclear profile function (NPF), $G(b)$, is available for study (see Fig. 3). This function contains all of the information for the scattering since it is, essentially, the Hankel transform of the amplitude (and since we are dealing only with spin-zero on spin-zero scattering there is only one amplitude). Clearly, the NPF is strongly dependent on the single-particle density and the general shape reflects this.

It is natural to ask about other characteristics of the nucleon distribution, such as short-, medium-, and long-range correlations. They must manifest themselves in some manner but how? One can get some feeling for this effect by considering the "anatomy" of the calculation. We see in Eq. (2) that the NPF is expressed as one minus a product. When this product goes to zero the NPF becomes unity, which corresponds to total absorption. When the impact parameter b is large, only one factor (at most) in the product will differ from unity and only the single-particle density matters. As b becomes smaller, more factors differ from one and the product becomes smaller in magnitude. Since the real part of the coefficient of the exponential in the function Γ, g, is less than unity over most of the range of energies treated here each factor has modulus less than one. The imaginary part, a_I, of a is smaller than the real part, a_R, and so plays a minor role in this qualitative discussion and we treat a as real for that reason.

Just how small each factor is depends on the distance $|\mathbf{s}_i - \mathbf{s}_j|$; if it is small then the factor is also small. This difference does not depend on nucleon-nucleon correlations since $\mathbf{s}_i$ and $\mathbf{s}_j$ are in different nuclei. However, since real g is of the order of 0.25–0.8, no one factor can drive the product to zero—it will take a combination of several factors. This will require that several nucleons be located close together and the probability of this occurring is sensitive to the correlations. Just how close together the nucleons have to be (in the two-dimensional space) is governed by a_R. Typical values of $\sqrt{a_R}$ are in the range of 1 fm. Repulsive correlations pushing the nucleons outside of this range would lead to greater transparency. Correlations shorter than this range can be expected to have little effect.

At the same time that the modulus of the product is decreasing it is developing a phase. Under the conditions just outlined, the phase of each factor has the same sign so the phase grows monotonically as each factor is included. Thus the behavior of the NPF depends on the relative sizes of the phase and the modulus of the product. If the phase reaches π while the modulus of the product is still sizable then the NPF will increase before becoming unity, as seen in Fig. 3 with the CMC included. Further changes leading to the average modulus becoming larger (with only modification of the phase) could even lead to oscillations.

In an effort to get a feeling for the effective number factors (and thus the number of times that the correction is being applied) we calculated the profile function for values of b in the crucial range of the surface as a function of the number of factors (see Fig. 4). As we progress from large to small values of b more factors are important. For large b the profile function can be expressed as a sum of first-order terms and

TABLE I. Parameters used in the calculations based on the nucleon-nucleon partial-wave amplitude analysis of Ref. [56].

Case	$T_{\rm Lab}$ (GeV) [Ref.]	$T_{\rm Lab}/A$ (MeV)	σ (mb)	ρ	a_R	a_I	$\theta^{\rm c.m.}_{\rm Max}$ (deg)	$-t_{\rm Max}$ [(GeV/c)^2]
^{6}He-^{12}C	0.230 [64]	38.3	163.5	0.680	14.6	− 8.06	20	0.139
^{6}He-^{12}C	0.250 [65]	41.6	159.7	0.737	16.0	− 7.91	10	0.038
α-^{16}O	0.240 [66]	60	103.2	0.953	20.8	− 6.65	12	0.051
^{16}O-^{16}O	1.120 [67,68]	70	86.4	1.049	23.0	− 5.87	22	1.224
α-^{208}Pb	0.288 [69]	72	83.0	1.069	29.2	− 4.85	33	0.700
α-^{208}Pb	0.340 [69]	85	65.0	1.169	25.7	− 4.85	30	0.686
^{12}C-^{12}C	1.016 [70]	85	65.0	1.169	25.7	− 4.85	18	0.560
^{16}O-^{40}Ca	1.503 [71]	94	60.5	1.185	26.3	− 4.56	6	0.254
^{16}O-^{12}C	1.503 [71]	94	60.5	1.185	26.3	− 4.56	15	0.565
α-^{16}O	0.400 [72]	100	57.5	1.196	26.7	− 4.36	37	0.800
α-^{208}Pb	0.480 [69]	120	47.4	1.233	28.1	− 3.70	20	0.443
^{12}C-^{12}C	1.449 [73]	120	47.4	1.233	28.1	− 3.70	12	0.356
^{12}C-^{12}C	1.620 [74]	135	43.1	1.212	28.6	− 3.84	12	0.398
α-^{208}Pb	0.699 [69]	175	36.2	1.095	29.2	− 5.05	12	0.240
^{12}C-^{12}C	2.400 [73]	200	34.3	0.991	28.7	− 6.42	10	0.410
α-^{40}Ca	1.37 [75]	343	29.7	0.435	20.5	− 12.6	12	0.414
α-^{12}C	1.37 [76]	343	29.7	0.435	20.6	− 12.6	21	0.799
α-α	2.554 [77]	638	38.9	0.010	10.5	− 8.10	23	0.765
α-α	4.20 [78]	1050	42.5	− 0.303	8.06	− 3.25	13	0.400
α-^{12}C	4.20 [79,80]	1050	42.5	− 0.303	8.06	− 3.25	11	0.716

the dependence on the number of factors becomes linear. Of course, in this limit there are no CMC since only first order in the density is involved.

E. Center-of-mass treatment

The scattering between two composite objects is treated in terms of the coordinate connecting their centers of mass so that the particles making up the nuclei must be centered appropriately. This is the problem of center of mass which must be appropriately addressed. The Monte Carlo method can provide the solution. Consider two methods of treating the c.m. motion. Each one provides a density in which the sum of all of the position vectors is zero but they are not (in general) equivalent. The first method relies on Gaussian densities and provides a correction factor to a scattering calculation made with an auxiliary density centered about a fixed origin.

Franco and Yin [6] used this first method, developed by Czyz and Maximon [81] (see also Ref. [82]), which works only when using Gaussian densities because the center of mass can be expressed as a factor in this case. To implement this method, a model is made in which a product of densities is assumed to be invariant under translation and using the algebraic identity

$$e^{-A\alpha^2R^2}e^{-\alpha^2(\mathbf{r}_1-\mathbf{R})^2}e^{-\alpha^2(\mathbf{r}_2-\mathbf{R})^2}e^{-\alpha^2(\mathbf{r}_3-\mathbf{R})^2}\cdots = e^{-\alpha^2r_1^2}e^{-\alpha^2r_2^2}e^{-\alpha^2r_3^2}\cdots = \rho_a(r_1)\rho_a(r_2)\rho_a(r_3)\ldots, \quad (7)$$

where $\mathbf{R}\equiv(\sum\mathbf{r}_i)/A$ is the center-of-mass coordinate and $\rho_a(r)$ is an auxiliary density with reference to a fixed origin. The expectation value in Eq. (1) can be taken over the auxiliary density (a calculation which is much easier) and the expectation value of the translationally invariant density obtained by dividing by the expectation value of the first factor on the left.

For the density used by Franco and Yin with $\rho_a(\mathbf{s}_i)\equiv\phi^2(\mathbf{s}_i)$,

$$|\chi(\{\mathbf{s}\})|^2 = N\delta\left(\frac{1}{A}\sum_j\mathbf{s}_j\right)\prod_{i=1}^{A}\rho_a(\mathbf{s}_i) = \frac{N}{(2\pi)^3}\int d\mathbf{Q}\, e^{i\sum_j\mathbf{Q}\cdot\mathbf{s}_j/A}\prod_{i=1}^{A}\rho_a(\mathbf{s}_i), \quad (8)$$

where N is a normalization factor. The single-particle density relative to the center of mass, such as that obtained from electron scattering (see Refs. [83–86] for corrections), for example, will be obtained, by integrating over all but one of the coordinates, as

$$\rho_s(\mathbf{s}_1)\equiv\int d\mathbf{s}_2d\mathbf{s}_3\ldots|\chi(\{\mathbf{s}\})|^2 = \frac{N}{(2\pi)^3}\int d\mathbf{Q}\, e^{i\frac{\mathbf{Q}\cdot\mathbf{s}_1}{A}}\rho_a(\mathbf{s}_1)\rho^{A-1}(\mathbf{Q}/A). \quad (9)$$

The Fourier transform of the single-particle density (in the c.m.) will be

$$\rho_s(q)\equiv\int d\mathbf{s}_1\, e^{i\mathbf{q}\cdot\mathbf{s}_1}\rho_s(\mathbf{s}_1) = \frac{N}{(2\pi)^3}\int d\mathbf{Q}\,\rho_a(\mathbf{q}+\mathbf{Q}/A)\rho_a^{A-1}(\mathbf{Q}/A) = \frac{A^3N}{(2\pi)^3}\int d\mathbf{Q}\,\rho_a(\mathbf{q}+\mathbf{Q})\rho_a^{A-1}(\mathbf{Q}). \quad (10)$$

Normalizing, we have

$$\rho_s(q) = \frac{\int d\mathbf{Q}\,\rho_a(\mathbf{q}+\mathbf{Q})\rho_a^{A-1}(\mathbf{Q})}{\int d\mathbf{Q}\,\rho_a^A(\mathbf{Q})}. \quad (11)$$

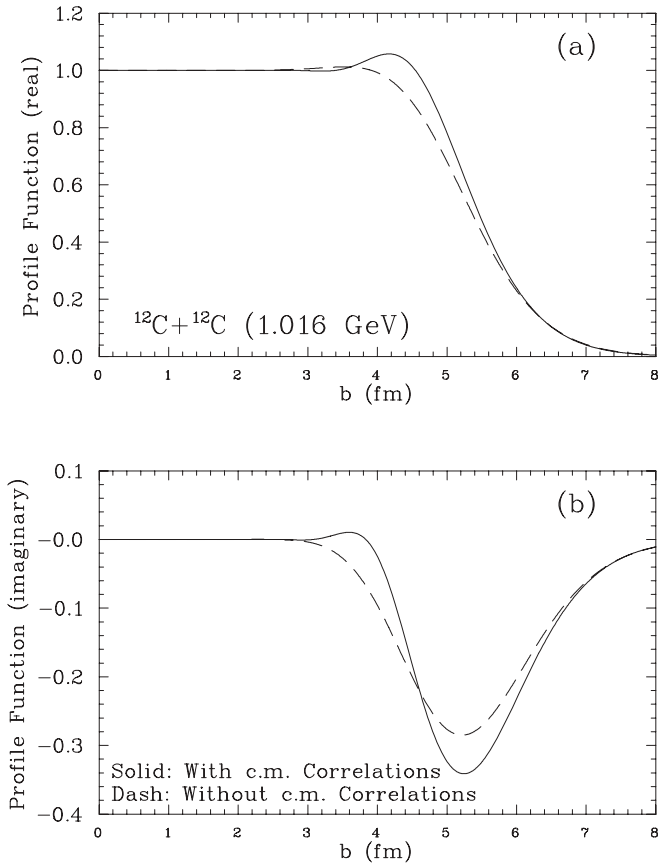

FIG. 3. The nuclear profile function for ^{12}C-^{12}C scattering with (solid) and without (dashed) center-of-mass correlations (CMC). The details of the calculation are discussed in Sec. III F.

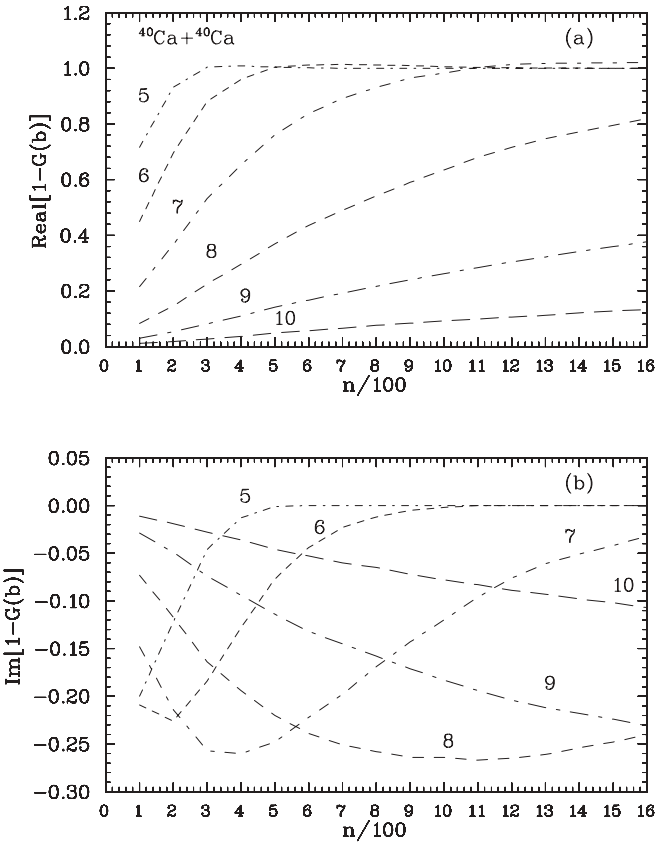

FIG. 4. One minus the accumulated nuclear profile function as a function of the number of factors in the product in Eq. (2) for ^{40}Ca-^{40}Ca scattering. The labels on the curves are the values of b in femtometers.

For a Gaussian form in momentum space as Franco and Yin [6] assumed,

$$\rho_a(p) = e^{-p^2/4\alpha^2}, \tag{12}$$

we can perform the integral on $\mathbf{Q}$ to find

$$\rho_s(q) = e^{-\frac{(A-1)q^2}{4A\alpha^2}}, \tag{13}$$

so that the auxiliary density has the same (Gaussian) form as the single-particle density but with a larger rms radius: $r_a^2 = Ar_s^2/(A-1)$.

We can also calculate the transform of the full density [Eq. (8)] in the general case as

$$\begin{aligned}\rho_s(\{\mathbf{q}\}) &\equiv \int d\mathbf{s}_1 d\mathbf{s}_2 \ldots d\mathbf{s}_A \, e^{i(\mathbf{q}_1\cdot\mathbf{s}_1+\mathbf{q}_2\cdot\mathbf{s}_2\cdots+\mathbf{q}_A\cdot\mathbf{s}_A)}|\chi(\{\mathbf{s}\})|^2 \\ &= \frac{N}{(2\pi)^3}\int d\mathbf{Q}\prod_{i=1}^{A}\rho_a(\mathbf{q}_i+\mathbf{Q}/A) \\ &= \frac{\int d\mathbf{Q}\prod_{i=1}^{A}\rho_a(\mathbf{q}_i+\mathbf{Q})}{\int d\mathbf{Q}\,\rho_a^A(\mathbf{Q})}.\end{aligned} \tag{14}$$

Evaluating with a Gaussian form we have

$$\rho_s(\{\mathbf{q}\}) = e^{-[\sum q_i^2 - \frac{1}{A}(\sum \mathbf{q}_i)^2]/4\alpha^2}. \tag{15}$$

In the Monte Carlo method the algorithm leading to a density in the center-of-mass frame is to first select the A coordinates, $\mathbf{u}$, according to A independent auxiliary densities, $\eta_a(u)$, (assumed to be isotropic). The functions $\eta_a(u)$ have chosen forms and the principal aim of this section is to develop a method to pick the functions $\eta_a(u)$ such that they result in a specified single-particle density relative to the center of mass. The coordinates to be used in the integration are obtained from the set of vectors $\mathbf{u}_i$ by

$$\mathbf{s}_i = \mathbf{u}_i - \frac{1}{A}\sum \mathbf{u}_j, \tag{16}$$

which means that the Monte Carlo densities that result from this transformation produce (by construction) functions whose vector coordinates sum to zero.

In summary, the procedure is to choose (isotropic) distributions according to density $\eta_a(u)$ for all of the nucleons in a given nuclear configuration. The center-of-mass vector is then computed and subtracted from each of the $\mathbf{u}_i$ to give the coordinates to be used in the evaluation of $G(\mathbf{b}, \{\mathbf{s}\}, \{\mathbf{s}'\})$.

In order to choose an auxiliary function that gives a particular center-of-mass density it is very useful to have explicit expressions for the two functions that we need to connect. The Fourier transform of the single-particle density

relative to the center of mass will be given by

$$\eta_s(q) = \int d\mathbf{u}_1 d\mathbf{u}_2 \ldots d\mathbf{u}_A \times e^{i\mathbf{q}\cdot(\mathbf{u}_1 - \frac{1}{A}\sum \mathbf{u}_j)} \eta_a(u_1)\eta_a(u_2)\ldots\eta_a(u_A) = \eta_a\left(\frac{A-1}{A}q\right)\eta_a^{A-1}\left(\frac{q}{A}\right). \quad (17)$$

To compare with the results of the previous section we can assume a Gaussian form again, i.e., $\eta_a(p) = e^{-p^2/4\beta^2}$, to get

$$\eta_s(q) = e^{-\frac{q^2}{4\beta^2}\frac{(A-1)^2}{A^2}} e^{-\frac{q^2}{4\beta^2}\frac{A-1}{A^2}} = e^{-\frac{A-1}{A}\frac{q^2}{4\beta^2}}, \quad (18)$$

which (by taking $\alpha = \beta$) gives the same result as the method used by Franco and Yin. For the full Fourier transform we have

$$\eta_s(\{\mathbf{q}\}) = \int d\mathbf{u}_1 d\mathbf{u}_2 \ldots d\mathbf{u}_A \times e^{i\sum_{i=1}^A \mathbf{q}_i\cdot\left(\mathbf{u}_i - \frac{1}{A}\sum_{j=1}^A \mathbf{u}_j\right)} \eta_a(u_1)\eta_a(u_2)\ldots\eta_a(u_A) = \int d\mathbf{u}_1 d\mathbf{u}_2 \ldots d\mathbf{u}_A \times e^{i\sum_{i=1}^A \mathbf{u}_i\cdot\left(\mathbf{q}_i - \frac{1}{A}\sum_{j=1}^A \mathbf{q}_j\right)} \eta_a(u_1)\eta_a(u_2)\ldots\eta_a(u_A) = \prod_{i=1}^A \eta_a\left(\mathbf{q}_i - \frac{1}{A}\sum_{j=1}^A \mathbf{q}_j\right). \quad (19)$$

If we take the Gaussian form again we have

$$\eta_s(\{\mathbf{q}\}) = e^{-\sum_{i=1}^A \left(\mathbf{q}_i - \frac{1}{A}\sum_{j=1}^A \mathbf{q}_j\right)^2/4\beta^2} = e^{-\left[\sum_{i=1}^A \mathbf{q}_i^2 - \frac{1}{A}(\sum_{i=1}^A \mathbf{q}_i)^2\right]/4\beta^2}. \quad (20)$$

which, with $\alpha = \beta$ again, is the same result as found previously. So we see that for Gaussian functions the two methods give identical results.

Equation (17) is general if all nucleons have the same density. For the case where the number of protons and neutrons is not equal and the neutrons and protons have different density shapes a different form holds. If $\zeta_a(q)$ is the Fourier transform of the proton auxiliary function and $\zeta_s(q)$ is the Fourier transform of the proton single particle in the center of mass [and $\eta_a(q)$ and $\eta_s(a)$ are the corresponding functions for the neutrons] then the functions will be related by

$$\zeta_s(q) = \zeta_a\left(\frac{A-1}{A}q\right)\zeta_a^{Z-1}\left(\frac{q}{A}\right)\eta_a^N\left(\frac{q}{A}\right), \quad (21)$$

$$\eta_s(q) = \eta_a\left(\frac{A-1}{A}q\right)\eta_a^{N-1}\left(\frac{q}{A}\right)\zeta_a^Z\left(\frac{q}{A}\right). \quad (22)$$

If the auxiliary functions for the protons and neutrons have rms radii R_{pa} and R_{na}, respectively, the corresponding radii for the center-of-mass densities will be related by

$$R_{pc}^2 = \left\{[(A-1)^2 + (Z-1)]R_{pa}^2 + NR_{na}^2\right\}/A^2, \quad (23)$$

$$R_{nc}^2 = \left\{[(A-1)^2 + (N-1)]R_{na}^2 + ZR_{pa}^2\right\}/A^2. \quad (24)$$

For the case of a given form chosen for the single-particle density, we need to find an auxiliary density which satisfies Eq. (17) or

$$\eta_a(q)\,\eta_a^{A-1}\left(\frac{q}{A-1}\right) = \eta_s\left(\frac{Aq}{A-1}\right). \quad (25)$$

One can find a solution to this equation for small q, by first expanding both $\eta_s(q)$ (assumed to be known) and $\eta_a(q)$ for small q:

$$\eta_a(q) = 1 - \mu q^2 \ldots, \quad \eta_s(q) = 1 - \nu q^2 \ldots. \quad (26)$$

Then we have to first order in q^2

$$(1-\mu q^2)[1-\mu q^2/(A-1)^2]^{(A-1)} = (1-\mu q^2)[1-\mu q^2/(A-1)] = 1 - \mu q^2\frac{A}{A-1} = 1 - \nu q^2\frac{A^2}{(A-1)^2}, \quad (27)$$

so that

$$\mu = \frac{\nu A}{A-1}, \quad (28)$$

and the same relation holds between the rms radii in the general (Monte Carlo) case as for the Gaussian case.

We could (in principle) solve Eq. (25) numerically on a mesh by constructing the first few elements on the mesh (three of them) with the expansion. Then we can continue to calculate the remaining values on the mesh by evaluating the ith point on the mesh with

$$\eta_a(q_i) = \eta_s\left(\frac{Aq_i}{A-1}\right)/\eta_a^{A-1}\left(\frac{q_i}{A-1}\right), \quad (29)$$

where the value of η_a in the denominator is obtained by interpolation from previously calculated values on the mesh. These values would always be available since the argument is much smaller. This process works well for a Gaussian form but is not stable when there is a zero in the form factor.

In practice, we choose parametrized forms for $\eta_a(q)$ and vary the parameters using Eq. (17) to fit an (assumed known) function, $\eta_s(q)$. For convenience we choose functions to represent $\eta_a(r)$ which can be readily sampled directly (see, e.g., Ref. [87]).

The density with the center-of-mass effect is distinguished from the product density with the same single-particle radial distribution by the fact that the distances between members of any pair of particles is greater than it would be for a simple product density. We can see this as follows.

For a single-particle density with independent particles the average of the square of the distance between particles is given by

$$\langle(\mathbf{r}_1 - \mathbf{r}_2)^2\rangle = 2\langle r^2\rangle - 2\langle\mathbf{r}_1\cdot\mathbf{r}_2\rangle = 2\langle r^2\rangle \quad (30)$$

since the average over the independent particles gives a cross term of zero. If we include a center-of-mass condition

$$\sum_{i=1}^A \mathbf{r}_i = 0 \quad (31)$$

then, replacing $\mathbf{r}_2$ in the cross product gives

$$\langle \mathbf{r}_1 \cdot \mathbf{r}_2 \rangle = -\langle r^2 \rangle - \sum_{i=3}^{A} \langle \mathbf{r}_1 \cdot \mathbf{r}_i \rangle$$
$$= -\langle r^2 \rangle - (A-2)\langle \mathbf{r}_1 \cdot \mathbf{r}_2 \rangle = -\frac{\langle r^2 \rangle}{A-1}. \quad (32)$$

Thus, with center-of-mass correlations

$$\langle (\mathbf{r}_1 - \mathbf{r}_2)^2 \rangle = 2\langle r^2 \rangle \frac{A}{A-1}. \quad (33)$$

For individual nuclear configurations we have

$$\frac{\sum_{i \neq j} (\mathbf{r}_i - \mathbf{r}_j)^2}{A(A-1)} = \frac{2A}{A-1} \frac{\sum_k r_k^2}{A}. \quad (34)$$

Thus we see that there is a correlation among pair of nucleons arising from the c.m. corrections. This condition is realized explicitly in the present method since the auxiliary density has a squared radius which is a factor of $A/(A-1)$ larger than the single-particle density in the center of mass and, since the positions are independently chosen, Eq. (30) holds with the larger square radius. Since the displacement of the density to satisfy the center-of-mass condition does not change the distance between nucleons, this larger interparticle distance is preserved while the distance of individual particles from the center of the nucleus is reduced.

With the procedure used here there is an initial density constructed in a Monte Carlo sense and then each realization is shifted by an amount to put the center of mass at the origin. In a spherical density with each particle thrown independently of the others, the rms distance between any pair of particles is $\sqrt{2}$ times the rms radius of the nucleus. Since the shift of the entire nucleus does not change the distance between pairs and the initial (auxiliary) density has a larger extent than the final density relative to the c.m. then the relative distance between pairs in the final density will be larger than the one which would be associated with a density constructed from independently thrown nucleons with the shape of the center-of-mass density. As the mass number A goes up this effect will become smaller with the relationship for the interparticle radius squared being $R^2_{\mathrm{CMC}} = A/(A-1) \times R^2_{\mathrm{No\ CMC}}$. Hence one might assume that the center-of-mass effect goes to zero as A increases.

While it is true that the basic effect is becoming smaller, the calculation of a given observable may not be. In the case that we are treating, of multiple scattering, the number of scatterings increases with A. Each scattering among the nucleons depends on the relative distance between nucleons and, while this distance is approaching that which would come from an independent particle density, the smaller effect is applied more times (i.e., there are more scatterings) so it is a numerical question as to whether the effect decreases or perhaps even increases with A. If the fundamental scattering interaction is weak so that only the low-order scatterings are important then one can expect that the effect decreases with A. However, for the strong NN interaction it is possible that the importance of the CMC to multiple scattering does not decrease with A at all. Consider, for instance, the case of the scattering of a nucleus with A nucleons on its twin. In this case the number of scatterings goes as A^2 although there will be other factors which will limit the effective number of scatterings.

F. Sampling considerations

The multidimensional integral in Eq. (1) is to be done using a Monte Carlo method. The function to be averaged over, $[G(b)]$, is complex but, as we shall see, the densities can be easily sampled. Ordinarily Monte Carlo methods are not very accurate if one takes a Fourier transform over a binned distribution (which we are not doing here). The integral in Eq. (3) is done by a standard quadrature method.

It is convenient to sample from pools of configurations of nuclei. For a variational or Monte Carlo Green's function method for generating the nuclei this is the natural way to carry out the sampling process, but even if direct sampling is being done it is a useful method. One creates N_t configurations for the target and N_p for the projectile. Then M samples are taken in pairs, one from each pool, of all of the nucleons for a nucleus from the same configuration. If M is large enough the pairs will be identical for some cases. However, the number of identical pairs will be $M^2/N_t N_p$ for a fraction of repeated pairs of $M/N_t N_p$. Thus for a typical case of 1 million entries in each pool and 10 million Monte Carlo samples the pairs repeat only $10^7/10^{12} = 1/10^5$ fraction of the time.

This technique is also useful for calculating the effect of no CMC. One can simply take the coordinates for each nucleon from a *different* configuration. This guarantees that the same single-particle center-of-mass density is used but the coordinates in each nuclear configuration are uncorrelated.

The auxiliary functions are chosen with a form which can be easily sampled. A common form used in many of the cases which follow is

$$r^2 \rho(r) = \sum g_n r^n \frac{b_n^{n+1} e^{-b_n r}}{n!}. \quad (35)$$

Often only two terms in the sum are needed to get an adequate representation. To sample this function one term is selected with probability g_n and then the corresponding normalized probability function is sampled. The functions in this case can be sampled easily by choosing r by

$$r = -\frac{\ln \prod_{i=1}^{n+1} X_i}{b}, \quad (36)$$

where the sets X_i comprise independent random numbers uniformly distributed between 0 and 1.

G. Coulomb correction

If the full amplitude with the Coulomb interaction is written as the divergent series

$$f(\theta) = \frac{1}{2ik} \sum_{\ell=0}^{\infty} (2\ell+1)(S_\ell - 1) P_\ell(\cos\theta) \quad (37)$$

then we can add and subtract the (divergent) series representation of the Rutherford amplitude

$$f_R(\theta) = \frac{1}{2ik}\sum_{\ell=0}^{\infty}(2\ell+1)(e^{2i\sigma_\ell}-1)P_\ell(\cos\theta) \quad (38)$$

to find a convergent series

$$f(\theta) = f_R(\theta) + \frac{1}{2ik}\sum_{\ell=0}^{\infty}(2\ell+1)(S_\ell - e^{2i\sigma_\ell})P_\ell(\cos\theta). \quad (39)$$

The total amplitude is now

$$f(\theta) = f_R(\theta) + \frac{1}{2ik}\sum_{\ell=0}^{\infty}(2\ell+1)e^{2i\sigma_\ell}(S_\ell e^{-2i\sigma_\ell}-1)P_\ell(\cos\theta), \quad (40)$$

where $f_R(\theta)$ is the Rutherford amplitude and the σ_ℓ are the Coulomb phase shifts. The amplitude without the Coulomb interaction is written as

$$f_0(\theta) = \frac{1}{2ik}\sum_{\ell=0}^{\infty}(2\ell+1)\left(S_\ell^0-1\right)P_\ell(\theta), \quad (41)$$

and we can write the factor between the two S-matrix elements as

$$C_\ell \equiv S_\ell e^{-2i\sigma_\ell}/S_\ell^0 \quad (42)$$

(see Ref. [42] and references therein). In this method the two S-matrix elements on the right-hand side are taken from an optical model fit with and without the Coulomb interaction. This correction is called the "inner" Coulomb correction; the "outer" correction corresponds to multiplication by the Coulomb S matrix. The procedure is then to calculate C_ℓ from Eq. (42) using for S_ℓ the result of an optical model fit with the full Coulomb interaction and for S_ℓ^0 the value from the same optical model without the Coulomb interaction. The quantity C_ℓ is then used as a correction factor with S_ℓ^0 coming from a partial-wave expansion of the Glauber amplitude and S_ℓ being the Coulomb-corrected result. That is,

$$S_\ell = C_\ell e^{2i\sigma_\ell} S_\ell^0, \quad (43)$$

where the S-matrix element on the left is the Coulomb-corrected Glauber result and S_ℓ^0 is the result from a Glauber model calculation (without any Coulomb interaction). The amplitude can then be calculated using Eq. (39) or (40).

Another way of getting the inner correction was given by Fäldt and Pilkuhn [43] as a shift in the value used in the integral over the profile function,

$$F(\mathbf{q}) = ik\int_0^\infty bdbJ_0(qb)G(b'), \quad (44)$$

where

$$b' = \sqrt{b^2+\eta^2/k^2}+\eta/k, \quad (45)$$

Here $\eta = ZZ'\alpha c/v$ is the Coulomb parameter and k is the center-of-mass momentum. The Coulomb-corrected S-matrix element will be given by

$$S_\ell = S_\ell^{FP} e^{2i\sigma_\ell}, \quad (46)$$

where S_ℓ^{FP} is the matrix element coming from the expansion of Eq. (44) in partial waves. For a similar method of treating the Coulomb correction see Vitturi and Zardi [88].

In order to carry out either of these corrections it is necessary to have the amplitude expressed as a partial-wave sum. Since the eikonal calculation gives the amplitude as a function of momentum transfer or angle the projection of the amplitude onto partial waves is needed. The projection was not made directly. By using Eq. (3) we can write

$$S_\ell - 1 = -k^2\int_{-1}^{1}dx\int_0^\infty bdbP_\ell(x)J_0[q(x)b]G(b). \quad (47)$$

The integral over x of $P_\ell(x)J_0[q(x)b]$ can be carried out first very efficiently (see Appendix A). The result was then integrated over b with $b\,G(b)$. As a check the amplitude was then reconstructed from the S-matrix elements and compared with the original calculation. With the method given in Appendix A agreement was found within 0.1%.

Figure 5 compares the two methods of making the inner correction for $^{16}O + {}^{16}O$ (see Sec. III H for details). It displays the ratio of the fully corrected amplitude to that with only the outer correction. It is remarkable how well the two methods agree. The disagreement beyond 16 degrees is due mainly to the fact that the optical model is calculated with a finite charge distribution and the method of Fäldt and Pilkuhn assumes a point charge distribution. For other treatments of the Coulomb correction, see Refs [89] and [90].

III. APPLICATION OF THE MONTE CARLO METHOD: RESULTS

In this section we carry out calculations using the full Glauber formalism with values of the parameters taken from fits to the nucleon-nucleon amplitudes [56]. In some cases we will vary those parameters to investigate the sensitivity to their values. Table I summarizes the cases treated, the data sources, and the free-space parameters used.

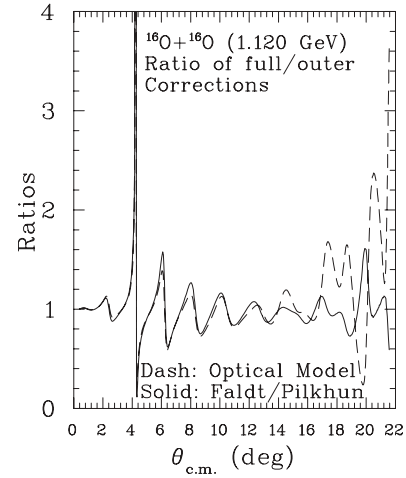

FIG. 5. The ratio of inner + outer corrections to outer corrections only for the Fäldt-Pilkuhn [43] (point Coulomb) and optical model with a realistic charge density. The full angular distributions are given in Sec. III H.

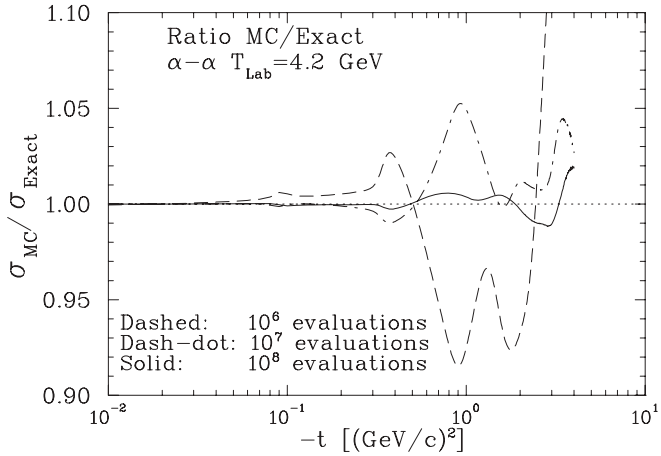

FIG. 6. Ratio of calculations for α-α scattering for different numbers of Monte Carlo evaluations showing the degree of calculational precision obtained. The α-particle density used is the same one used by Franco and Yin [6].

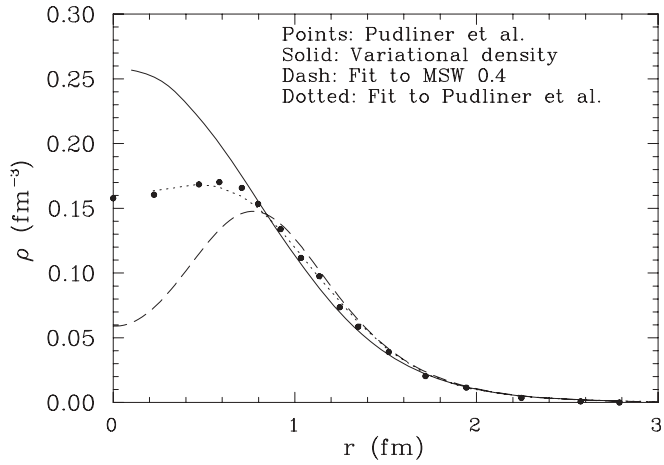

FIG. 7. Comparison of three densities used for the α particle in the calculations. The reference MSW is to McCarthy, Sick, and Whitney [91]. The points were read from Fig. 15 in Pudliner *et al*. [3].

A. α-α scattering

There are some interesting points for the α-α scattering calculation. Notice that there is no separate center-of-mass correction factor as there was in the formulation of Franco and Yin [6]. The Monte Carlo method calculates directly using the many-body density with the method outlined above. As a test of the method we repeat the calculation of Franco and Yin [6] using their technique and the Monte Carlo method using Gaussian densities. From the previous discussion on the center-of-mass correction we should expect to find the same result aside from Monte Carlo statistical errors. Figure 6 shows the ratios of the calculations done in these two ways. It is seen that the results are the same to about 2% even though the absolute magnitude of the cross section changes by almost 10 orders of magnitude over the angular range considered. The difference between the two calculations is invisible on a log scale. For 10^8 Monte Carlo evaluations the calculation took about 10 h on a standard 2.5-GHz personal computer.

The nucleon density of ^{4}He has been somewhat of a puzzle. The fits to electron scattering [91] with the method of a sum of Gaussians (SOG) show a large depression in the center of the nucleus that the Monte Carlo Green's function calculations do not exhibit [3]. However, the χ^2 per data point is considerably less than unity, showing that perhaps an overfit was present in the SOG fit. By using other forms to represent the density, acceptable fits with a significantly smaller depression can be found. We have made a fit to the electron-scattering data [91] with a density in which we constrained the ratio of the density at the origin to that at the peak to be 0.4 in order to have a density similar to that found in Ref. [91] but with a less severe depression. That density is shown in Fig. 7 as the dashed line. We fit this density to find an auxiliary density given by

$$r^2\rho_{\rm MSW}(r) = (1-\alpha)N_1(e^{-a_e r} - e^{-b_e r})^{10} + \alpha\left[0.95N_2 e^{-(r-r_0)^2/a_0^2} + 0.05N_3 e^{-(r-r_1)^2/a_1^2}\right], \quad (48)$$

where $\alpha = 0.43$ and

$$a_e = 0.51\ \text{fm}^{-1}, \quad b_e = 0.61\ \text{fm}^{-1}, \quad r_0 = 1.28\ \text{fm}, \quad r_1 = 1.8\ \text{fm}, \quad a_0 = 0.1\ \text{fm}, \quad a_1 = 0.3\ \text{fm}. \quad (49)$$

N_1, N_2, and N_3 are chosen to normalize each of the individual probability densities. The calculations of Pudliner *et al*. [3] give perhaps the best estimate of the ^{4}He density and show only a slight depression in the central region. Also shown in Fig. 7 is a fit to the Monte Carlo density of Pudliner *et al*. [3] (large dots) from reading the points from the graph. The auxiliary density for this fit is given by

$$r^2\rho_{\rm Pud} = \lambda_4 d^{15} r^{14} e^{-dr}/14! + (1-\lambda_4) f^9 r^8 e^{-fr}/8!, \quad (50)$$

where $\lambda_4 = 0.835$ and the resulting density is shown in Fig. 7 (dotted line). In order to have a density with short-range correlations included we have carried out our own variational calculation (see Appendix B).

To test for the relative importance of the short-range correlations and the center-of-mass correlations, we performed the calculation as outlined in the previous section starting from the single-particle density resulting from a density derived from a binning of the variational result. The c.m. density from that calculation is also shown in Fig. 7 (solid line).

The auxiliary density, $\eta_a(r)$, as fit to the variational density can be expressed as

$$r^2\eta_{\rm Var}(r) = (1-\alpha)g_1(r) + \alpha g_2(r), \quad (51)$$

where

$$g_1(r) = N_g r^2 e^{-a_g r^2}, \quad g_2 = N_e(e^{-a_e r} - e^{-b_e r})^2, \quad \alpha = 0.505, \quad a_g = 0.56\ \text{fm}^{-2}, \quad a_e = 0.779\ \text{fm}^{-1}, \quad b_e = 1.345\ \text{fm}^{-1}, \quad (52)$$

where N_g and N_e were chosen to normalize g_1 and g_2 individually. Note that the volume element, r^2, is included in each case. Since the wave function has an asymptotic limit of the form $e^{-\kappa r}/r$ then, with the volume element included, the tail should behave as an exponential.

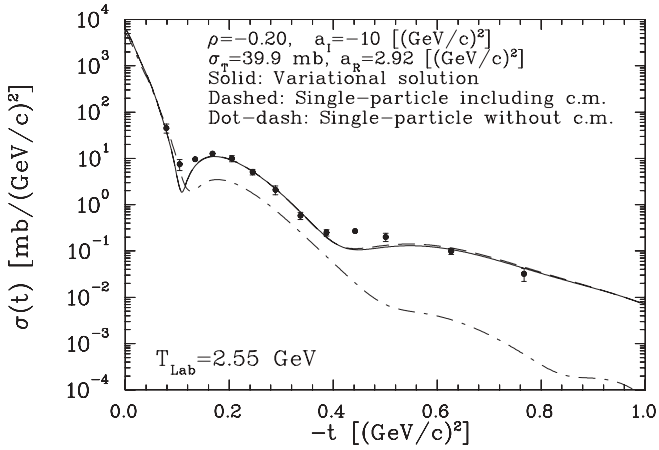

FIG. 8. Calculations of α-α scattering showing the effect the center-of-mass correlations. The dash-dot curve uses the same Metropolis density as the solid curve but each nucleon is drawn from a different (random) realization of the nucleus. Thus it has the same single-particle density but the effect of the CMC is missing. The data are from Berger *et al*. [77].

Figure 8 shows a test of the importance of short-range correlations and center-of-mass correlations. For this illustration only, the parameters have been chosen to give a reasonable representation of the data, unlike most other figures presented which use the free parameters determined from amplitude analyses [56]. The solid curve shows the calculation with the full variational wave function and the dashed curve shows the results obtained with the auxiliary density used to correct for the center of mass. The dash-dot curve shows the result of choosing each nucleon from a different configuration of the nucleus. In this case the single-particle density will be identical to the other two cases but there are no CMC among the nucleons. The principal difference between the two is that the solid curve does not have the short-range correlations that are in the variational wave function. Hence, at least for the variational calculation performed here (see Appendix B), they are not important in agreement with Ullo and Feshbach [93].

Figure 9 shows the dependence on the density used. It is seen that the sensitivity is very small and reasonable variations would not seem to be able to significantly improve the agreement with the data.

Figure 10 shows a comparison of the calculation at a beam energy of 4.2 GeV with the data of Satta *et al*. [78]. Also shown are the results of a variation with the ρ parameter. This parameter is the least well determined experimentally of the nucleon-nucleon parameters. It is seen that the prediction is rather poor when compared with the data and that moderate variations of ρ are unlikely to improve the agreement.

B. α-^{12}C scattering

The carbon auxiliary density was obtained from the modified harmonic oscillator fit of charge density obtained from electron scattering data [92]. The form found for the auxiliary density is

$$r^2\eta_{12}(r) = 0.90916\, h_1(r) + 0.09084\, h_2(r), \qquad (53)$$

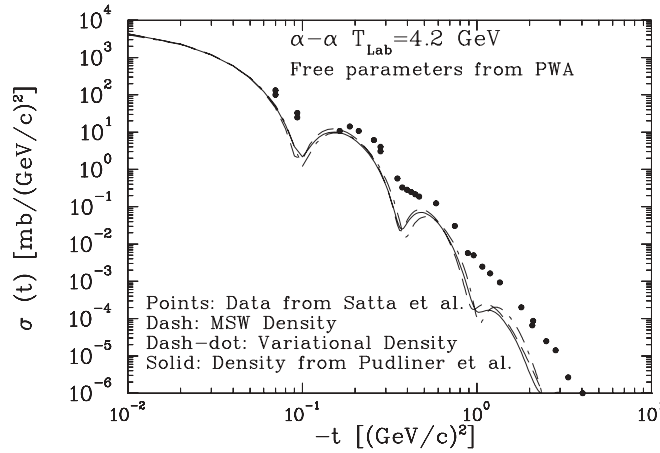

FIG. 9. α-α scattering at $T_{\rm Lab} = 4.2$ GeV showing the dependence on the density used. The notation MSW refers to the fit to the electron scattering fit by McCarty, Sick, and Whitney [91] as described in the text. The partial wave analysis (PWA) is that of Ref. [56]. The data are from Satta *et al*. [78].

where

$$h_1(r) = M_1 r^{10} e^{-d_{12}r}, \quad h_2(r) = M_2(e^{-a_{12}r} - e^{-b_{12}r})^2, \qquad (54)$$

$d_{12} = 0.7311$ fm^{-1}, $a_{12} = 1.7488$ fm^{-1}, and $b_{12} = 0.6429$ fm^{-1}. M_1 and M_2 are chosen to normalize h_1 and h_2 separately.

Figure 11 shows the auxiliary density and the center-of-mass body and charge densities which result. For the light nuclei the auxiliary density is normally quite different from the center-of-mass density.

Figure 12 shows the variation of the differential cross section at 4.2 GeV with the parameter ρ. As for α-α scattering at the same energy (Fig. 9) the moderate variations of ρ do not improve the agreement with the data. Figure 13 shows the prediction for α-^{12}C scattering at 1.37 GeV kinetic energy with a variation of the parameter a_I. The agreement is no better than that at 4.2 GeV. Variations of the other parameters give

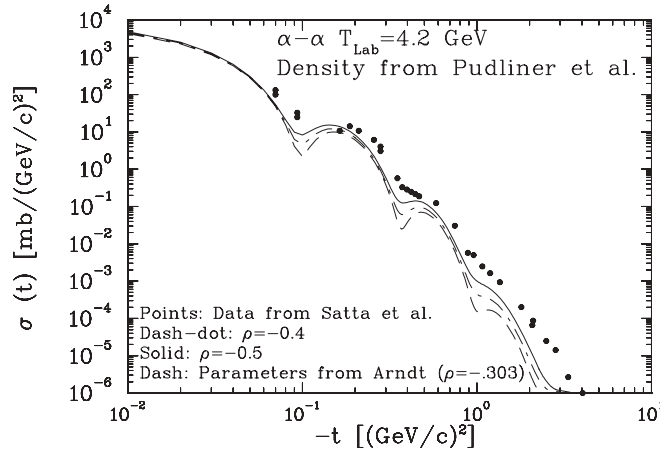

FIG. 10. α-α scattering at 4.2 GeV showing the variation with the parameter ρ. The data are from Satta *et al*. [78]. PWA means the partial wave analysis from Ref. [56].

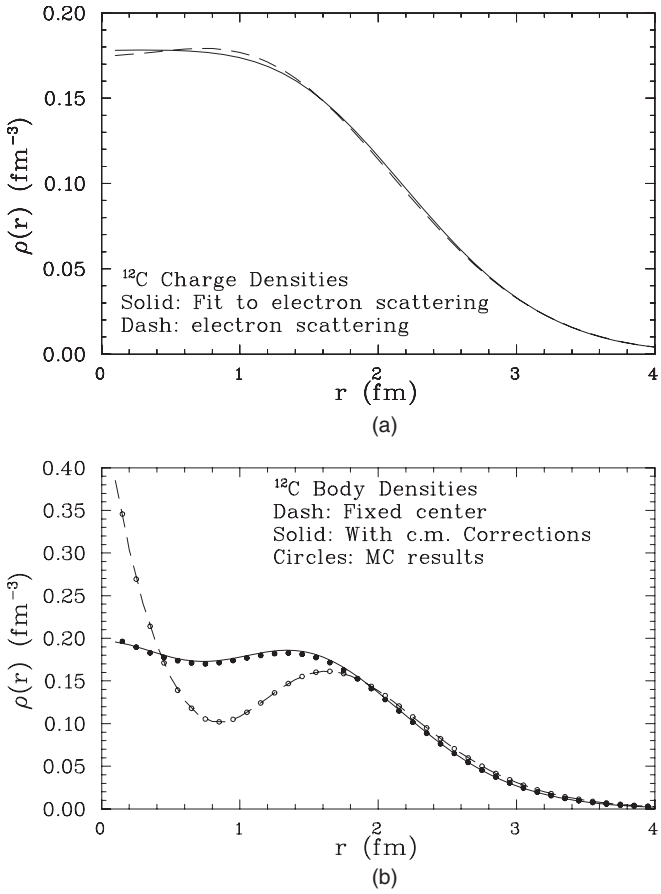

FIG. 11. (a) The fit to the ^{12}C charge density using the auxiliary density in Eq. (53). The electron-scattering data are from Ref. [92]. (b) The point density along with the auxiliary density. Also shown are the points obtained from binning the radius values in the Monte Carlo calculation, with the open circles corresponding to the auxiliary density and the solid circle to the center-of-mass density.

similar results. Again, it seems unlikely that a modest variation in parameters will bring the calculation in line with the data.

C. α-^{16}O scattering

The auxiliary function for ^{16}O was taken to have the form

$$r^2\eta_{16}(r) = 0.8646\, v_1(r) + 0.1354\, v_2(r), \qquad (55)$$

with

$$v_1(r) = M_1 r^{10} e^{-d_{16}r}, \quad v_2(r) = M_2(e^{-a_{16}r} - e^{-b_{16}r})^2, \qquad (56)$$

and

$$a_{16} = 2.738\ \text{fm}^{-1},\ b_{16} = 0.2976\ \text{fm}^{-1},\ d_{16} = 4.174\ \text{fm}^{-1}, \qquad (57)$$

with

$$M_1 = d_{16}^{11}/10!$$

and

$$M_2 = 2a_{16}b_{16}(a_{16} + b_{16})/(a_{16} - b_{16})^2$$

chosen to normalize v_1 and v_2.

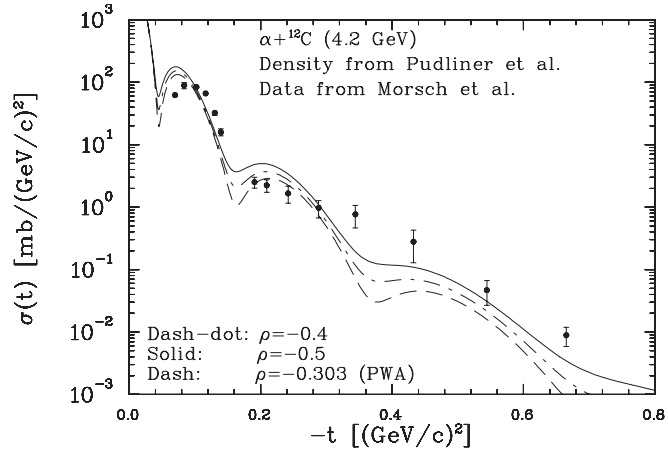

FIG. 12. α-^{12}C scattering at 4.2 GeV showing the variation with the parameter ρ. The data are from Morsch *et al.* [79,80]. PWA means the partial wave analysis from Ref. [56].

Figure 14 shows the results of the α-^{16}O calculation compared with the data of Wakasa *et al.* [72] at 400 MeV. Here the agreement at forward angles is satisfactory. Figure 15 compares the calculation at 240 MeV with the data of Lui *et al.* [66]; here the agreement is fairly good (aside from a slight normalization problem) up to about 7 degrees. After that there is a considerable difference. The Coulomb correction is substantial, especially at larger angles.

D. α-^{40}Ca scattering

The auxiliary density for Ca was obtained from a point density extracted from pion scattering [94] which is very similar to that obtained from electron scattering [95]. The form of the auxiliary density is

$$r^2\eta_{40}(r) = 0.740072\, v_1(r) + 0.259928\, v_2(r), \qquad (58)$$

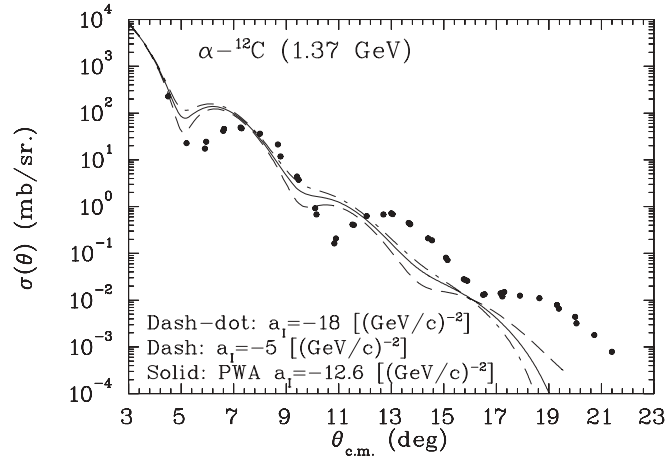

FIG. 13. Comparison of α-^{12}C scattering with data of Chaumeaux *et al.* [76] showing the effect of a variation of the nucleon-nucleon parameter a_I. PWA refers to the partial wave analysis of Ref. [56]. The density for the α projectile is taken from Pudliner *et al.* [3] as described in the text.

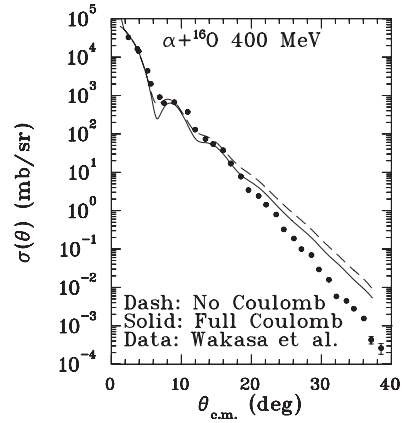

FIG. 14. Comparison of α-^{16}O scattering with data of Wakasa *et al*. [72] showing the effect of the Coulomb correction.

with

$$v_1(r) = M_1 r^{10} e^{-d_{40} r}, \quad v_2(r) = M_2 (e^{-a_{40} r} - e^{-b_{40} r})^2, \tag{59}$$

and

$$a_{40} = 0.641 \text{ fm}^{-1}, \; b_{40} = 0.443 \text{ fm}^{-1}, \; d_{40} = 3.597 \text{ fm}^{-1}, \tag{60}$$

with M_1 and M_2 chosen to normalize v_1 and v_2.

The results of a calculation for α-^{40}Ca scattering at 1.37 GeV are shown in Fig. 16 and compared to the data of Alkhazov *et al*. [75]. The Coulomb correction plays a very large role. There would be no agreement at all without it. While the agreement is far from perfect, it is satisfactory for no adjustable parameters at least for angles less than 8 degrees (with the exception of the two forward data points which have large errors). For other treatments of α-^{40}Ca scattering see Refs. [96] and [97].

E. α-^{208}Pb scattering

The auxiliary density for ^{208}Pb was fit to the charge density of ^{208}Pb so it corresponds to the proton density. It is believed that the neutron density is different from the proton density but

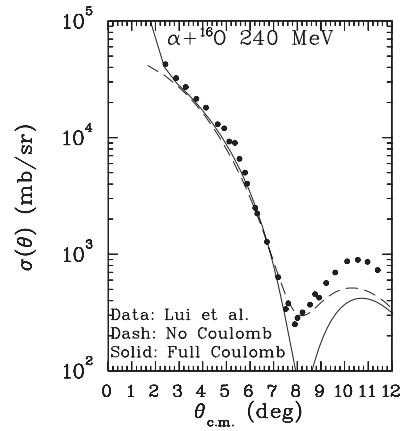

FIG. 15. α-^{16}O scattering at 240 MeV. The data are from Lui *et al*. [66].

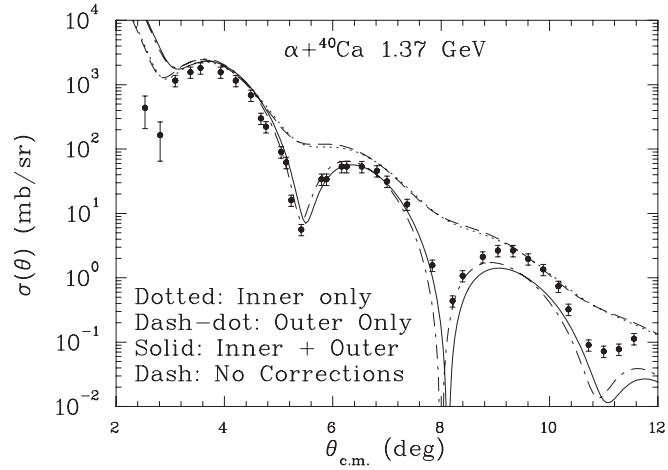

FIG. 16. α-^{40}C scattering at 1.37 GeV compared with the data of Alkhazov *et al*. [75].

a study of the effect of a different neutron density, interesting though it might be, is beyond the scope of the present work. Since the lead nucleus is much larger than the other nuclei considered so far, with a significant flat portion of the density inside the surface, the forms of the auxiliary density used for the lighter nuclei are not appropriate for this case. Because of the large number of nucleons, the difference between the auxiliary density and the center-of-mass density is not very great. For these reasons a Woods-Saxon (WS) density fit to the charge density was used [98]. The volume element must be included as well in the sampling, as has been done in previous cases. While the WS density can be directly sampled, it is the form

$$r^2 \rho_{Pb}(r) \propto \frac{r^2}{1 + e^{\left(\frac{r-c}{a}\right)}} \tag{61}$$

which is needed. This sampling was done by the method of selection of variables [87]. A comparison was made between variables from two samples. First, r_1 is chosen according to a linear distribution from 0 to R_0; then a second value, r_2, was obtained from the WS distribution with

$$r_2 = a \ln \left\{ \frac{1}{b[(1 + 1/b)^F - 1]} \right\},$$

where F is a random number uniformly distributed between 0 and 1 and $b = e^{-c/a}$. If r_2 is greater than r_1 it returned as the desired value of r. Otherwise the process is repeated. The α-particle density used was the one fit to Pudliner *et al*. [3] as discussed earlier.

Figure 17 shows the results of calculations at energies of 288, 340, 480, and 699 MeV compared with the data of Bonin *et al*. [69]. The Coulomb correction plays a very large role in determining the cross section, as might be expected. The agreement is rather good in the forward direction but worsens rapidly beyond a certain angle, in a fashion that is different for each energy.

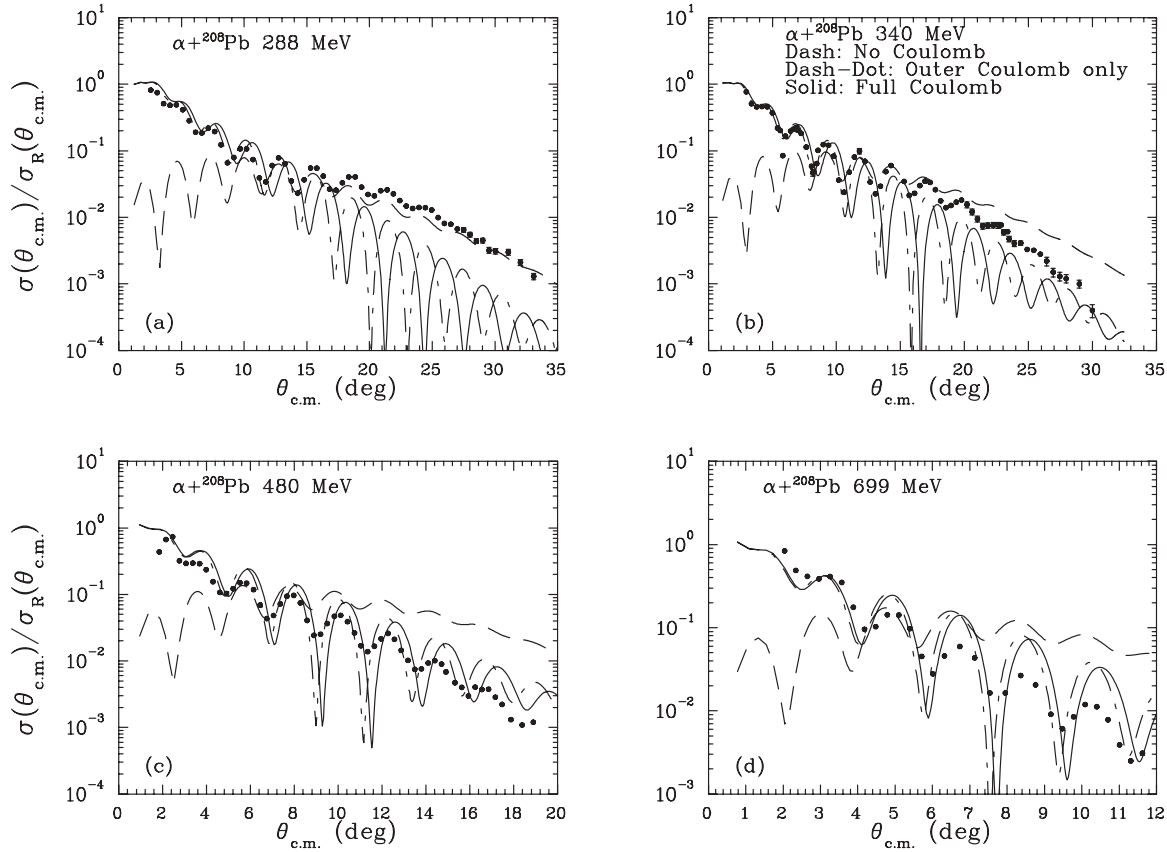

FIG. 17. α-^{208}Pb scattering compared with the data of Bonin *et al.* [69].

F. ^{12}C-^{12}C scattering

A comparison with the data at 1.016 GeV [70] and 1.45 and 2.4 GeV [73] has been been made by several groups [14,16,20, 22,23,25,26,48,99–101] using various methods. See also the phase-shift analysis by Mermaz *et al.* [102]. We can use the ^{12}C densities found in Sec. III B to calculate the scattering of ^{12}C from ^{12}C.

We have carried out a test of the size of the center-of-mass effect in much the same way as was done for the variational wave function in α-α scattering earlier. The scattering calculations just presented were made by repeating the realization (in a Monte Carlo loop) of two carbon nuclei and then carrying out the evaluation of the necessary equations. The calculation can also be done by first constructing a pool of nuclei, each properly centered about the center of mass (with one million being used in the current calculation), and then drawing complete nuclei randomly from this pool for each carbon nucleus. These two methods give the same result.

One can now modify the calculation, in the same manner as before, so as to choose the 12 different vector coordinates for each carbon nucleus from 12 different realizations in the pool. In this way one is guaranteed to have the same single-particle density but with uncorrelated particles. The result of a calculation for this energy with a spherical density for ^{12}C is shown in Fig. 18 where it is seen that both the Coulomb and center-of-mass corrections play a large role. The agreement is good up to an angle of about 5 degrees [$t \approx -0.045$ (GeV/c)^2] but poorer after that.

The result without center-of-mass corrections is shown as the dashed curve. While this curve is shown as the ratio to the Rutherford amplitude as a function of angle and Fig. 8 for helium gives the absolute cross section as a function of t, one can see that the effect is very similar in the two cases. Thus, at least for this very limited sample of two cases, the center-of-mass effect does not decrease.

Figure 3 shows the profile function for ^{12}C for the cases with and without CMC. One can understand the behavior to some extent. For small values of b the many factors in the

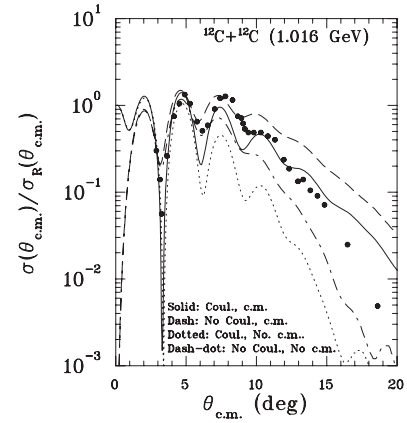

FIG. 18. ^{12}C-^{12}C scattering at 1.016 GeV with and without the center-of-mass correction. The data are from Buenerd *et al.* [70].

product in Eq. (2) (144 for the case of ^{12}C-^{12}C scattering), a large fraction of which have magnitude less that unity, will cause it to be very small. This very small correction to unity leaves the profile function at essentially one in this region of b, and hence it is insensitive to the CMC.

On the other hand, for large b one can expand the product in terms of single, double, triple, etc. scatterings. Since double scattering will have two factors of the Gaussian function, triple scattering will have three factors, etc., single scattering will dominate for large b. Since we are holding the single-particle density in the c.m. fixed, the CMC will have no effect in this region. Because the large b values dominate the forward scattering we must expect the small-angle cross section to be insensitive to the CMC, as is observed.

Thus, it is only in a relatively small region of values of b that the effect will be influential. From Fig. 3 this is for $3.5 < b < 5.5$ fm. Since, as one decreases b from the external region the sensitivity to the CMC will become greater as the number of scatterings goes up until this number gets to be so large that the product becomes very small in magnitude.

It is generally believed that carbon has a strong oblate deformation. Lesniak and Lesniak [103] included this effect in proton-carbon scattering using Glauber theory. While they developed the proper, fully quantum theory, in the end they used a semiclassical approximation, simply averaging the amplitude over rotated densities (see also Ref. [104]). Some recent studies (of fission and reactions [105]) have treated the problem in the same way. As pointed out in Ref. [103], electron scattering (at least in the single-interaction approximation) should not depend on the deformation so the average density remains the same as before. We assume a form for the density symmetric about the z axis and with a distribution in the polar angle given by

$$\rho(r,\theta) \propto \rho_0(r)\sin^n\theta. \tag{62}$$

This simple form is inspired by considerations from Ref. [106] (p. 62). The paper of Svenne and Mackintosh [107] presented arguments why ^{12}C was known to be deformed in response to the paper by Friar and Negele [108] who pointed out that, with the usual form of the deformed density, the existence of a deformation for ^{12}C was contrary to the electron scattering measurements since the falloff of the density in the surface region was strongly affected. The form of Eq. (62) does not suffer from this problem, as can be seen by taking the example of $n = 2$. In this case we have

$$\begin{aligned}\rho(r,\theta) &\propto \rho_0(r)\sin^2\theta \propto \frac{2}{3}\rho_0(r)[1 - P_2(\cos\theta)]\\ &= \rho_0(r)\left(\frac{2}{3} - \frac{8\pi}{15}\sum_m Y_2^m(\theta_p,\phi_p)Y_2^{m*}(\theta_a,\phi_a)\right),\end{aligned} \tag{63}$$

where the Legendre polynomial has been expanded in terms of angles relative to a fixed axis. Here (θ_p, ϕ_p) are angles of a given nucleon in the nucleus with respect to a fixed axis and the angles (θ_a, ϕ_a) are those of the body symmetry axis relative to the same fixed axis. With a one-body operator the second term will give a $j_2(qr)$ transform of the density but when the average over the direction of the body axis of the carbon nucleus is taken it will vanish. Hence a one-body operator probes only the "spherical part" of the density.

For $n = 2$ the probability in θ is given by

$$\rho(\theta) = \tfrac{3}{4}\sin^2\theta, \tag{64}$$

which leads to

$$\langle z^2\rangle = \tfrac{1}{5}\langle r^2\rangle, \quad \langle x^2\rangle = \langle y^2\rangle = \tfrac{2}{5}\langle r^2\rangle, \quad \langle x^2\rangle/\langle z^2\rangle = 2. \tag{65}$$

For $n = 4$ the probability in θ is given by

$$\rho(\theta) = \tfrac{15}{16}\sin^4\theta, \tag{66}$$

which leads to

$$\langle z^2\rangle = \tfrac{1}{7}\langle r^2\rangle, \quad \langle x^2\rangle = \langle y^2\rangle = \tfrac{3}{7}\langle r^2\rangle, \quad \langle x^2\rangle/\langle z^2\rangle = 3. \tag{67}$$

These densities look more like donuts than ellipsoids of revolution (if one assumes that this density is applied to all the nucleons and not just the p shell). We note that α cluster models would also lead to densities with zero at the center. We can estimate the β_2 parameter describing deformation by using prescriptions given by Hagino [109] based on the rms radii.

We take

$$\gamma \equiv \frac{\langle x^2\rangle^{\frac{1}{2}}}{\langle z^2\rangle^{\frac{1}{2}}} = \frac{1 - \frac{1}{2}\beta_2\sqrt{\frac{5}{4\pi}}}{1 + \beta_2\sqrt{\frac{5}{4\pi}}} \tag{68}$$

so that

$$\beta_2 = \frac{1-\gamma}{\frac{1}{2}+\gamma}\sqrt{\frac{4\pi}{5}}. \tag{69}$$

For $n = 2$, we have $\beta_2 = -0.34$, and for $n = 4$, $\beta_2 = -0.52$. Svenne and Mackintosh [107] gave a survey of values obtained for β_2. From their list we see that the Nilsson model gives $\beta_2 = -0.64$ and the α cluster model gives $\beta = -0.41$. A little later Vermeer *et al.* [110] measured the quadrupole moment of the 2^+ state from which one can infer a quadrupole moment for the ground state of $-22 \pm 10\ e\,\text{fm}^2$, implying a value of $\beta_2 = -0.57$ with a 50% error. In a recent calculation of ^{12}C-^{12}C fusion [105] the value $\beta_2 = -0.4$ was used (along with a hexadecapole term). Thus, these forms lead to reasonable values of the deformation.

The results for $n = 2$ and $n = 4$ are shown in Fig. 19 and compared with data. Again it is seen that agreement with data is good in the forward direction but deteriorates rapidly at larger angles. The deformation plays a significant role at larger angles.

G. ^{16}O-^{12}C scattering

The scattering of oxygen on carbon is shown in Fig. 20. The effect of the correction for the Coulomb interaction is quite large. For the same scattering the effect of the correction for the center of mass is also shown. It is seen that the agreement at very forward angles is very good with the Coulomb correction playing a substantial role. While it cannot be said that the agreement with data is good at larger angles, the calculation follows the trend of the data quite well, which is not true if either the Coulomb or center-of-mass correction is not included.

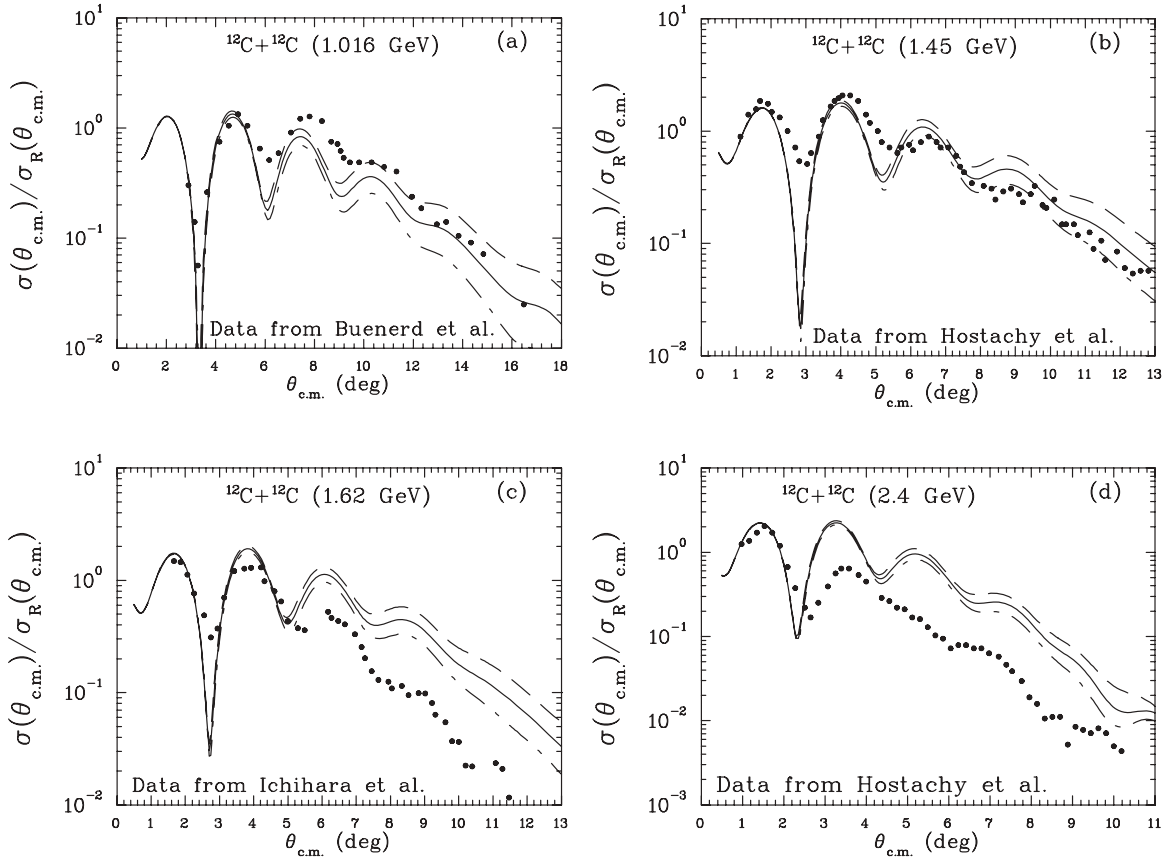

FIG. 19. Comparison of three deformations of the carbon nucleus at four energies. The dashed curves correspond to a spherical nucleus ($n = 0$), the solid curve to a ratio of 1.14 ($n = 2$), and the dash-dot curve to a ratio of 1.73 ($n = 4$). The data are from Buenerd *et al*. [70], Hostachy *et al*. [73], and Ichihara *et al*. [74].

H. ^{16}O-^{16}O scattering

Using the density found earlier we calculated oxygen scattering from oxygen at 1.120 GeV. The comparison with the data of Nuoffer *et al*. [67] is shown in Fig. 21. For angles beyond 5 degrees there is a considerable discrepancy (and even more after the Coulomb correction) but inside of that angle the agreement is quite good.

In order to test the inner Coulomb correction we made an optical-model fit to the data [67]. A simple form was used:

$$V_{\rm opt}(r) = -\frac{V_0}{1+e^{(r-r_R)/a_R}} - \frac{iW_0}{1+e^{(r-r_I)/a_I}}, \qquad (70)$$

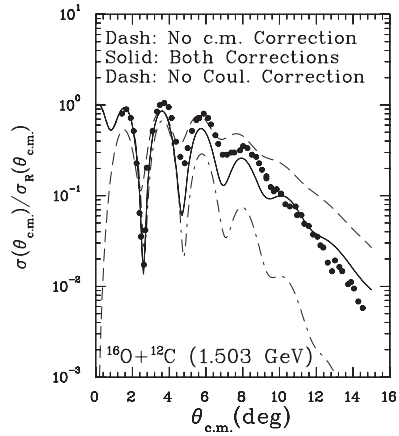

FIG. 20. The ^{16}O-^{12}C scattering cross section showing the effect of the Coulomb and center-of-mass corrections. The data are from Roussel-Chomaz *et al*. [71].

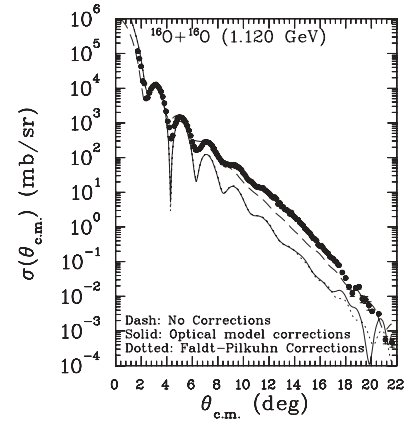

FIG. 21. ^{16}O-^{16}O scattering at 1.12 GeV. The data are from Nuoffer *et al*. [67] and Khoa *et al*. [68].

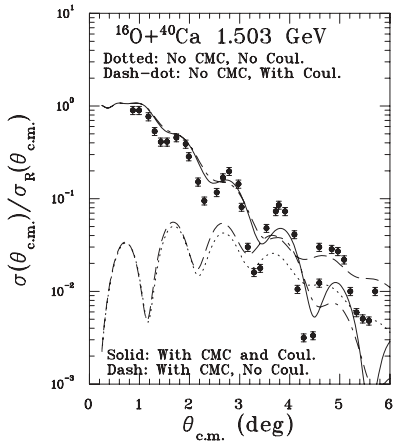

FIG. 22. The ^{16}O-^{40}Ca scattering cross section showing the effect of the Coulomb and c.m. corrections. The data are from Roussel-Chomaz *et al*. [71].

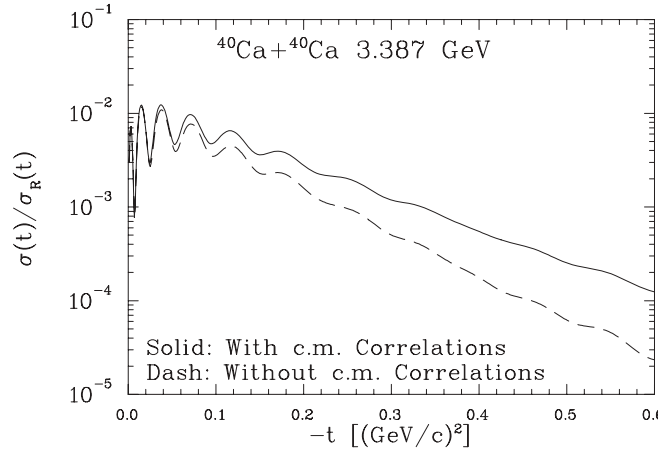

FIG. 23. The ratio of the ^{40}Ca-^{40}Ca cross section to the Rutherford cross section at 3.387 GeV using the appropriate parameters from Ref. [56] for this energy.

with $r_R = 2r_R^0(16)^{\frac{1}{3}}$ and $r_I = 2r_I^0(16)^{\frac{1}{3}}$. A uniform charge density with a radius $r_q = 2. \times 1.3 \times (16)^{\frac{1}{3}}$ was used. The fit parameters were $V_0 = 150.4$ MeV, $r_R^0 = 0.784$ fm, $a_R = 0.897$ fm, $W_0 = 44.4$ MeV, $r_I^0 = 1.005$ fm, and $a_I = 0.745$ fm. By calculating with and without the Coulomb interaction, a Coulomb correction can be obtained by the method shown in Eq. (42). Alternatively, we can make the correction with the method of Fäldt and Pilkuhn [43] by modifying the integral over the profile function. As seen in Fig. 5 the results are nearly identical over most of the angular range.

I. ^{16}O-^{40}Ca scattering

The result of ^{16}O-^{40}Ca scattering is shown in Fig. 22 and compared with data of Roussel-Chomaz *et al*. [71]. Again one sees the importance of the center-of-mass and Coulomb corrections. The agreement at forward angles is moderately good but is considerably worse at larger angles. For another treatment of this reaction at this energy see Ref. [111].

J. ^{40}Ca-^{40}Ca scattering

Figure 23 shows the cross section for ^{40}Ca-^{40}Ca scattering at a kinetic energy of 3.387 GeV. There are no data to compare with and if there were they would be dominated by pure Coulomb interactions. In this case there are 1600 factors in the product in Eq. (1), which, if expanded in multiple scattering as was done in the paper by Franco and Yin [6], would give $2^{1600} \approx 4 \times 10^{481}$ terms. The calculation is shown to illustrate the fact that, even for these medium-heavy nuclei, the center-of-mass correction remains important. We see that the effect of the CMC is not very different from the effect of CMC found in carbon-carbon scattering and is as large as a factor of 5. Since the basic CMC effect is the order of 1/40 in this case it is important to understand how many times it enters in to the calculation. See Sec. II D for a discussion of this point.

K. ^{6}He-^{12}C scattering

The Pudliner density for ^{6}He [3] was represented by two auxiliary functions (one for protons and one for neutrons) following Eqs. (21) and (22). The proton auxiliary density was given by

$$r^2\rho_p(r) = 0.273776\frac{r^{15}b_p^{16}e^{-b_p r}}{15!} + 0.726224\frac{r^8 c_p^9 e^{-c_p r}}{8!}, \tag{71}$$

with

$$b_p = 14.3466\ \text{fm}^{-1} \text{ and } c_p = 4.7125\ \text{fm}^{-1}, \tag{72}$$

and the neutron auxiliary density by

$$r^2\rho_n(r) = 0.208969\frac{r^{14}e_n e^{15}e^{-e_n r}}{14!} + 0.791031\frac{r^2 f_n^3 e^{-f_n r}}{2!}, \tag{73}$$

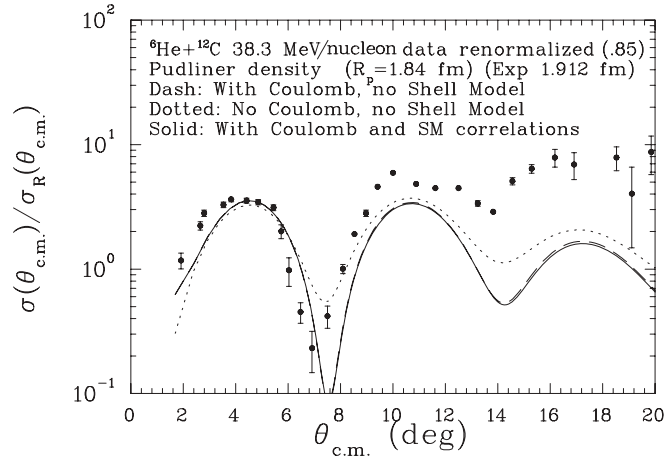

FIG. 24. ^{6}He-^{12}C scattering at 38.3 MeV/nucleon using the ^{6}He density from Pudliner *et al*. [3]. The data are from Lapoux *et al*. [64]. The experimental determination of the proton radius is from Ref. [112].

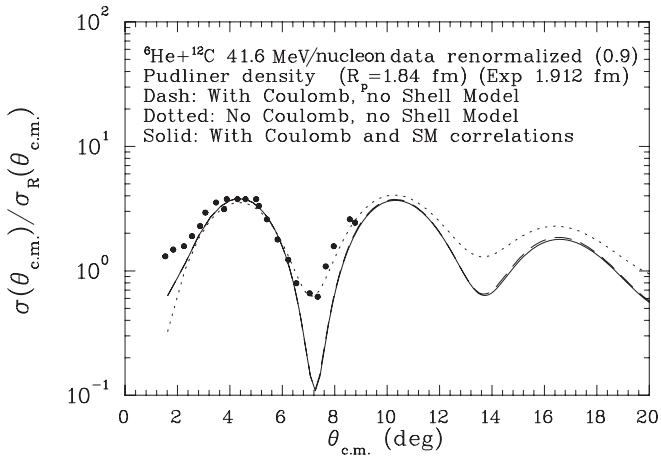

FIG. 25. ^{6}He-^{12}C scattering at 41.6 MeV/nucleon using the ^{6}He density from Pudliner *et al.* [3]. The data are from Al-Khalili *et al.* [65].

where

$$e_n = 5.72753\ \text{fm}^{-1} \text{ and } f_n = 1.65566\ \text{fm}^{-1}. \quad (74)$$

A "shell model" correlation was (optionally) included by coupling two $j = \frac{3}{2}$ neutrons to zero total angular momentum, which results in a factor in the density of

$$\tfrac{1}{2}(1 + \cos^2\theta_R), \quad (75)$$

where θ_R is the relative angle between the two valence neutrons. This factor was carried as a weight in the Monte Carlo calculation so that the calculations with and without the factor can be done in the same run. Figures 24 and 25 show the results for the calculation of ^{6}He-^{12}C scattering. It is seen that the effect of the shell-model correlation is very small. The Coulomb correction plays a significant role even for these low-Z nuclei. Perhaps a part of the reason for this is that the correlation is only between two of the six particles.

IV. DISCUSSION

The Glauber approximation can fail for a number of reasons not necessarily associated with the basic assumptions. These reasons include the following:

(i) At low energies the Fermi motion may cause significant corrections to the fixed-nucleon approximation.
(ii) The double spin flip in the nucleon-nucleon interaction which has been neglected may require a significant correction if the isospin constraints are not sufficient to eliminate it.
(iii) The single spin flip (occurring an even number of times) may become important for sufficiently large angles.
(iv) At high energies the coherent production of mesons constitutes an additional inelastic channel which is beyond the Glauber approximation.
(v) At small impact parameters there should be significant corrections to the nucleon-nucleon interactions because of the higher nuclear densities.
(vi) Correlations from the shell model are of the same range as those from the center of mass and may play a role as the nuclear penetration becomes greater.

In looking over the comparisons with data presented in the paper it is seen that often there is a forward region

TABLE II. Critical values of the angles and their equivalents in momentum transfer. Also given is the energy in the center of mass available for coherent meson production. The last four cases have no critical values listed because all data points available have a momentum transfer $\geqslant$1 fm^{-1}. The ^{6}He-^{12}C cases have not been included since it is not possible to claim agreement in the forward direction without absolute data.

Case	T_{Lab} (GeV) [Ref.]	θ_C (deg)	q_C (fm^{-1})	q_C^2 (GeV/c)^2	$\sqrt{s} - m_T - m_P$ (GeV)	Figure
α-^{208}Pb	0.288 [69]	8	1.04	0.042	0.28	17
α-^{208}Pb	0.340 [69]	7	0.99	0.038	0.33	17
α-^{208}Pb	0.480 [69]	5	0.85	0.028	0.47	17
α-^{208}Pb	0.699 [69]	4.5	0.93	0.034	0.65	17
^{16}O-^{12}C	1.503 [71]	4	1.02	0.041	0.64	20
^{16}O-^{16}O	1.120 [67,68]	5	1.28	0.064	0.55	21
^{16}O-^{40}Ca	1.503 [71]	2.5	1.06	0.044	1.06	22
^{12}C-^{12}C	1.016 [70]	4.5	0.96	0.036	0.50	18
α-^{16}O	0.240 [36]	7	0.66	0.017	0.19	15
α-^{16}O	0.400 [72]	7	0.89	0.031	0.32	14
^{12}C-^{12}C	1.449 [73]	4	1.01	0.040	0.71	19
^{12}C-^{12}C	1.620 [74]	3	0.80	0.025	0.80	19
^{12}C-^{12}C	2.400 [73]	2	0.66	0.017	1.17	19
α-^{40}Ca	1.37 [75]	8	2.18	0.184	1.23	16
α-^{12}C	4.20 [79,80]				2.87	12
α-^{12}C	1.37 [76]				0.99	13
α-α	2.55 [77]				1.18	8
α-α	4.20 [78]				1.87	9

where the prediction is moderately good (and sometimes quite good) followed by a more-or-less sudden transition to a poor agreement. Perhaps the best example of this is the scattering of α particles from ^{208}Pb (see Fig. 17). The transition is seen to take place at 8° at 288 MeV, 7° at 340 MeV, 5° at 480 MeV and 4.5° at 699 MeV. These angles and the corresponding momentum transfer and values of $-t$ are shown in Table II. All of the transition points are seen to correspond to a momentum transfer of about 1 fm^{-1} [$-t = 0.04(\mathrm{GeV}/c)^2$]. For ^{16}O-^{12}C scattering (see Fig. 20) the transition angle is about 4°, which corresponds to a momentum transfer of 1.01 fm^{-1}. For ^{16}O-^{16}O scattering (Fig. 21) the transition angle is around 5°, corresponding to a momentum transfer of 1.28 fm^{-1}. For ^{16}O-^{40}Ca scattering (Fig. 22) the transition angle is about 2.5°, which corresponds to a momentum transfer of 1.06 fm^{-1}. The remainder of the cases studied are shown in Table II as well and show a similar effect.

Figure 26 shows that at $q_C = 1$ fm^{-1} for the momentum transfer the interior of the nucleus is sampled. So $q_C = 1$ fm^{-1} does not seem to correspond to the onset of the nuclear matter being probed.

ACKNOWLEDGMENTS

We thank Dr. H. G. Bohlen for providing tables of the ^{16}O-^{16}O data and Dr. V. Lapoux for communicating to us the ^{6}He-^{12}C data at 38.2 MeV. WRG thanks the staff of Laboratoire de Physique Nucléaire et de Hautes Énergies for support during visits when part of this work was done.

APPENDIX A: PARTIAL-WAVE PROJECTION

We make the partial wave projection from the formula

$$\frac{1}{2ik}\sum_{\ell=0}^{\infty}(2\ell+1)(S_\ell-1)P_\ell(\cos\theta) = ik\int_0^\infty bdbJ_0(qb)G(b), \tag{A1}$$

where $q^2 = 2k^2(1-\cos\theta)$. In order to make this projection it is useful to have the expansion

$$J_0(qb) = \sum_{\ell=0}^{\infty} h_\ell(kb)P_\ell(\cos\theta). \tag{A2}$$

From Ref [113] 9.1.79 we have

$$J_0(qb) = J_0^2(kb) + 2\sum_{n=1}^{\infty} J_n^2(kb)\cos n\theta. \tag{A3}$$

In order to get the desired expression we need the expansion

$$\cos n\theta = \sum_{\ell=0}^{\infty} a_{n,\ell}P_\ell(\cos\theta), \tag{A4}$$

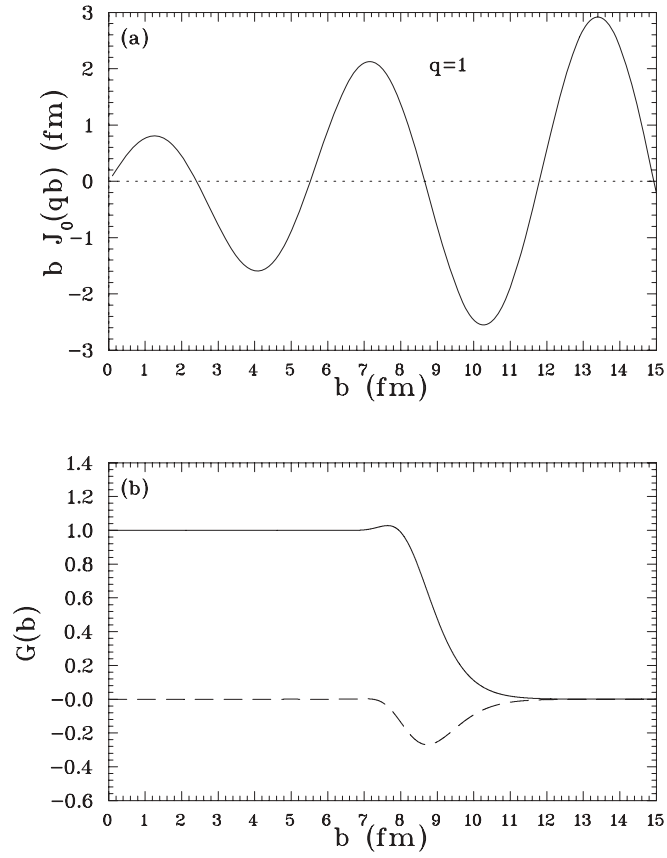

FIG. 26. (a) The factor of the kernel $bJ_0(qb)$ which represents the weighting of the nuclear profile function and (b) the nuclear profile function for α-^{208}Pb.

which actually cuts off at $\ell = n$ as we shall see. With the use of De Moivre's theorem one can see

$$\cos n\theta = \frac{1}{2}\sum_{m=0}^{n}\binom{m}{n}[i^m + (-i)^m]\sin^m\theta\cos^{n-m}\theta$$
$$= \sum_{m=even}^{n}\binom{m}{n}(-1)^{\frac{m}{2}}\sin^m\theta\cos^{n-m}\theta, \tag{A5}$$

where $\binom{m}{n}$ is the binomial coefficient. With $k = m/2$

$$\cos n\theta = \frac{1}{2}\sum_{m=0}^{n}\binom{m}{n}[i^m + (-i)^m]\sin^m\theta\cos^{n-m}\theta$$
$$= \sum_{k=0}^{\frac{n}{2}}\binom{2k}{n}(-1)^k(\sin^2\theta)^k\cos^{n-2k}\theta$$
$$= \sum_{k=0}^{\frac{n}{2}}\binom{2k}{n}(-1)^k(1-\cos^2\theta)^k\cos^{n-2k}\theta$$
$$= \sum_{k=0}^{\frac{n}{2}}\sum_{j=0}^{k}\binom{2k}{n}(-1)^k(-1)^j\binom{j}{k}\cos^{n-2k+2j}\theta.$$

With $m = n - 2k + 2j$ so that $m = n, n-2, n-4, \ldots$

$$\cos n\theta = \frac{1}{2}\sum_{m=0}^{n}\binom{m}{n}[i^m + (-i)^m]\sin^m\theta\cos^{n-m}\theta$$
$$= \sum\binom{n-m-2j}{n}(-1)^{\frac{n-m}{2}}\binom{j}{\frac{n-m}{2}-j}\cos^m\theta$$
$$= \sum c_{n,m}\cos^m\theta.$$

Thus we see that $\cos n\theta$ can be expanded in powers of $\cos\theta$ with powers of the same parity as n with maximum power n. We can now use the integral of a Legendre polynomial over a power of x (Ref. [113] 8.14.15),

$$\int_{-1}^{1} P_\ell(x)x^m dx = \frac{\pi^{\frac{1}{2}}2^{-m}\Gamma(1+m)}{\Gamma\left(1+\frac{1}{2}m-\frac{1}{2}\ell\right)\Gamma\left(\frac{1}{2}\ell+\frac{1}{2}m+\frac{3}{2}\right)} = d_{m,\ell}. \tag{A6}$$

Note that this integral is zero if ℓ and m are not of the same parity or if $\ell > m$.

We can write the expression for the $a_{n,\ell}$ as

$$a_{n,\ell} = \left(\ell+\frac{1}{2}\right)\sum_{\ell\leqslant m\leqslant n, m-n \text{ even}} c_{n,m}d_{m,\ell}. \tag{A7}$$

This expression was coded and the coefficients were calculated in this way; it works but the terms for different powers of $\cos\theta$ get very large and cancel in the sum so, even with double precision, one is limited to n of the order of 35 for small values of ℓ, which is not enough for our problem. The values for $n = \ell$ and other values of ℓ close to n are always calculated correctly. A useful check is

$$\sum_{\ell=0}^{n} a_{n,\ell} = 1, \tag{A8}$$

which follows from Eq. (A4) with $\theta = 0$.

However, there is a much easier way to get the coefficients needed. Using the trigonometric identity

$$\cos n\theta = 2\cos(n-1)\theta\cos\theta - \cos(n-2)\theta \tag{A9}$$

and the recursion relation for the Legendre polynomials,

$$xP_\ell(x) = \frac{\ell P_{\ell-1}(x) + (\ell+1)P_{\ell+1}(x)}{2\ell+1}, \tag{A10}$$

we find

$$\int_0^\pi \cos n\theta P_\ell(\cos\theta)\sin\theta d\theta \equiv b_{n,\ell}$$
$$= \frac{2}{2\ell+1}[\ell b_{n-1,\ell-1} + (\ell+1)b_{n-1,\ell+1}] - b_{n-2,\ell}. \tag{A11}$$

Since $a_{n,\ell} = \frac{2\ell+1}{2}b_{n,\ell}$ we have

$$a_{n,\ell} = \frac{2\ell a_{n-1,\ell-1}}{2\ell-1} + \frac{2(\ell+1)a_{n-1,\ell+1}}{2\ell+3} - a_{n-2,\ell} \tag{A12}$$

with the conditions

$$a_{0,0} = 1, \quad a_{1,1} = 1, \tag{A13}$$

and

$$a_{n,\ell} = 0 \tag{A14}$$

if n and ℓ are not of the same parity or if $\ell > n$. All values of these coefficients can be quickly calculated using the recursion relation (A12) without any numerical problem. Using these values then we obtain

$$h_0(kb) = J_0^2(kb) + 2\sum_{n=1}^{\infty} J_n^2(kb)a_{n,0}, \tag{A15}$$

$$h_\ell(kb) = 2\sum_{n=\ell}^{\infty} J_n^2(kb)a_{n,\ell}, \quad \ell > 0. \tag{A16}$$

$J_0(x)$ and $J_1(x)$ are calculated to one part in 10^7 and the recursion relation for Bessel functions is used for fixed b to obtain the higher values of n. Just beyond $n = bk$, the magnitude of $J_n(x)$ decreases rapidly and the recursion relation fails shortly thereafter. The recursion is cut off when $J_n^2(x)$ is less than 10^{-6}.

The functions $h_\ell(kb)$ have some interesting and potentially useful properties. For example, starting from Eq. (A2) with

$$\int_0^\infty J_0(qb)J_0(q'b)bdb = \delta^{(2)}(q-q')$$
$$= \frac{\delta(q-q')}{q} = 2\delta(q^2-q'^2) = \frac{1}{k^2}\delta(x-x') \tag{A17}$$

one can show that

$$\int_0^\infty h_\ell(y)h_{\ell'}(y)ydy = \frac{2\ell+1}{2}\delta_{\ell,\ell'}. \tag{A18}$$

Once the functions $h_\ell(bk)$ have been found, the process can be reversed; i.e., we can find the nuclear profile function for any given set of matrix elements. First from the inverse Hankel transform we have

$$G(b) = \frac{1}{ik}\int_0^\infty F(q)J_0(qb)qdq. \tag{A19}$$

Since the amplitude is assumed to fall off rapidly we can replace the upper limit with a finite, but large, one, namely $2k$ so that

$$G(b) \approx \frac{1}{ik}\int_0^{2k} F(q)J_0(qb)qdq. \tag{A20}$$

Changing the integration variable to $u \equiv q^2$ we have

$$G(b) \approx \frac{1}{2ik}\int_0^{4k^2} F(\sqrt{u})J_0(qb)du. \tag{A21}$$

Now changing the integration variable to $x = \cos\theta$ we have

$$G(b) \approx \frac{2k^2}{2ik}\int_{-1}^{1} A(x)J_0(q(x)b)dx, \tag{A22}$$

where $A(x) = F[q(x)]$ and

$$A(x) = \frac{1}{2ik}\sum_{\ell=0}^{\infty}(2\ell+1)(S_\ell-1)P_\ell(x). \tag{A23}$$

Using Eq. (A2) we have

$$G(b) \approx -\sum_{\ell=0}^{\infty}(S_\ell-1)h_\ell(kb). \tag{A24}$$

APPENDIX B: VARIATIONAL DENSITY FOR ^{4}He

One can solve for the ^{4}He wave function by Monte Carlo Green's function methods [2,3]. In this case either the walkers represent a probability proportional to the wave function itself (hence the walkers do not give the density needed for our scattering problem) or, if one uses importance sampling, then the walkers represent the product of the trial wave function and the true wave function and thus are more suitable for representing the density. In the work here we will use a variational trial wave function where the walkers represent directly the density to calculate α-α scattering.

Varga *et al*. [34] performed Monte Carlo calculations using a Metropolis sampling of a ^{4}He wave function obtained with Green's function Monte Carlo methods. We will make a comparison between the method given previously and a simplified version of this type of calculation based on the variational algorithm.

The variational method operates with the estimator of the energy given by

$$E_T = \frac{\int d\mathbf{R}\psi_T^*(\mathbf{R})(T+V)\psi_T(\mathbf{R})}{\int d\mathbf{R}\psi_T^*(\mathbf{R})\psi_T(\mathbf{R})} = \frac{\int d\mathbf{R}\rho(\mathbf{R})\left(\frac{T\psi_T(\mathbf{R})}{\psi_T(\mathbf{R})}+V\right)}{\int d\mathbf{R}\rho(\mathbf{R})}, \tag{B1}$$

where $\mathbf{R}$ represents the set of coordinates which describe the system. Using the Metropolis algorithm to represent the density, it is automatically normalized. The trial wave function is assumed to depend on some number of parameters and, upon varying these parameters the minimum energy achieved is guaranteed to be greater than or equal to the true ground state energy of the system. The trial wave function normally is expected to give a good representation of the true wave function but there is no guarantee of that.

In order to calculate with a realistic wave function we use a trial wave function which results from the following variational calculation for ^{4}He. Since the true wave function must be translationally invariant it can depend only on the six relative coordinates, $\mathbf{r}_{ij} = \mathbf{r}_i - \mathbf{r}_j$.

We choose the form

$$\psi(\mathbf{r}_1,\mathbf{r}_2,\mathbf{r}_3,\mathbf{r}_4) = \prod_{j>i} f(r_{ij}), \tag{B2}$$

where $r_{ij} = |\mathbf{r}_{ij}|$ and the function $f(r)$ is arbitrary at this point. It will be chosen with a number of parameters to be selected to minimize the energy. We can evaluate the kinetic energy needed as

$$\sum_{i=1}^{4}\frac{\nabla_i^2\psi(\mathbf{r}_1,\mathbf{r}_2,\mathbf{r}_3,\mathbf{r}_4)}{\psi(\mathbf{r}_1,\mathbf{r}_2,\mathbf{r}_3,\mathbf{r}_4)} = 2\sum_{j>i}\left(\frac{f''(r_{ij})}{f(r_{ij})}+2\frac{f'(r_{ij})}{r_{ij}f(r_{ij})}\right) + 2\sum_{[i,j,k]}\mathbf{r}_{ij}\cdot\mathbf{r}_{ik}\frac{f'(r_{ij})f'(r_{ik})}{r_{ij}r_{ik}f(r_{ij})f(r_{ik})}. \tag{B3}$$

The values of the three indices in the last sum are [123], [124], [134], [213], [214], [234], [312], [314], [324], [412], [413], and [423]. They can be obtained with nested loops,

$$\{i=1,4[j=1,3;j\neq i(k=j+1,4;k\neq i)]\}. \tag{B4}$$

With such a form it is relatively easy to calculate the kinetic energy since one only needs to be able to calculate the function f and its first and second derivatives. The derivatives can be calculated numerically if need be.

We took for the form of f such that

$$f(r) = (1-e^{-cr})\frac{e^{-ar}}{b+r}. \tag{B5}$$

The first factor vanishes at the origin and provides the effect of a (very mild) repulsive correlation. The rest of the function has the proper asymptotic form with the constant b avoiding the singularity at the origin.

We used a modified version [87] of the Malfliet-Tjon [114] potentials since we are neglecting spin in this calculation. The variational calculation overbinds ^{4}He by about 7 MeV (35 instead of 28 MeV) so we increased the strength of the repulsive part of the modified Malfliet-Tjon potentials (by 6%) in order to have a more realistic binding.

The variational calculation for the energy was carried out using 100 000 walkers. It was found that the energy was not very sensitive to the parameter b so it was fixed at 1.0 fm. Then, for various fixed values of c, the energy was calculated as a function of a. For the fixed values of b and c the rms radius is a unique function of a. We used $a = 0.203$ fm^{-1} and $c = 1.0$ fm^{-1}. The rms radius is a crucial parameter in the scattering and we obtained a value of 1.44 fm. The calculation was repeated 10 times to give a collection of one million walkers to use in the scattering calculations involving the α particle.

The coordinates needed for the scattering calculation were taken from the Metropolis algorithm every 2000 steps to be certain that each realization was independent. One million realizations of the helium density were calculated and written out to files. When the scattering was calculated, the coordinates of each nucleus were drawn from a nuclear representation chosen randomly from the pool of one million possible nuclear realizations.

[1] D. M. Ceperley and M. H. Kalos, in *Applications of the Monte Carlo Methods in Statistical Physics*, edited by K. Binder (Springer-Verlag, Berlin, 1984).
[2] J. Carlson, Phys. Rev. C **36**, 2026 (1987); **38**, 1879 (1988).
[3] B. S. Pudliner, V. R. Pandharipande, J. Carlson, S. C. Pieper, and R. B. Wiringa, Phys. Rev. C **56**, 1720 (1997).
[4] C. W. Johnson, S. E. Koonin, G. H. Lang, and W. E. Ormand, Phys. Rev. Lett. **69**, 3157 (1992),
[5] J.-P. Dedonder and W. R. Gibbs, Phys. Rev. C **69**, 054611 (2004).

[6] V. Franco and Y. Yin, Phys. Rev. Lett. **55**, 1059 (1985); Phys. Rev. C **34**, 608 (1986).
[7] Y. Yin, Z. Tan, and K. Chen, Nucl. Phys. A **440**, 685 (1985).
[8] B. Abu-Ibrahim, K. Fujimura, and Y. Suzuki, Nucl. Phys. A **657**, 391 (1999).
[9] J. S. Al-Khalili, I. J. Thompson, and J. A. Tostevin, Nucl. Phys. A **581**, 331 (1994).
[10] J. S. Al-Khalili and J. A. Tostevin, Phys. Rev. Lett. **76**, 3903 (1996).
[11] J. S. Al-Khalili and J. A. Tostevin, Phys. Rev. C **57**, 1846 (1998).
[12] J. S. Al-Khalili, J. A. Tostevin, and J. M. Brooke, Phys. Rev. C **55**, R1018 (1997).
[13] M. M. H. El-Gogary, Phys. Rev. C **68**, 054609 (2003).
[14] M. M. H. El-Gogary, A. S. Shalaby, M. Y. M. Hassan, and A. M. Hegazy, Phys. Rev. C **61**, 044604 (2000).
[15] V. Franco and G. K. Varma, Phys. Rev. C **18**, 349 (1978).
[16] M. M. H. El-Gogary, A. S. Shalaby, and M. Y. M. Hassan, Phys. Rev. C **58**, 3513 (1998).
[17] W. Horiuchi, Y. Suzuki, B. Abu-Ibrahim, and A. Kohama, Phys. Rev. C **75**, 044607 (2007); **76**, 039903(E) (2007).
[18] H. X. Zhong, Phys. Rev. C **51**, 2700 (1995).
[19] S. K. Charagi and S. K. Gupta, Phys. Rev. C **56**, 1171 (1997).
[20] B. Abu-Ibrahim and Y. Suzuki, Phys. Rev. C **62**, 034608 (2000).
[21] B. Abu-Ibrahim, Y. Ogawa, Y. Suzuki, and I. Tanihata, Comput. Phys. Commun. **151**, 369 (2003).
[22] B. Abu-Ibrahim and Y. Suzuki, Nucl. Phys. A **706**, 111 (2003).
[23] B. Abu-Ibrahim and Y. Suzuki, Phys. Rev. C **61**, 051601 (2000).
[24] V. Franco and W. T. Nutt, Phys. Rev. C **17**, 1347 (1978).
[25] S. M. Lenzi, A. Vitturi, and F. Zardi, Phys. Rev. C **40**, 2114 (1989).
[26] S. M. Lenzi, F. Zardi, and A. Vitturi, Nucl. Phys. A **536**, 168 (1992).
[27] A. M. Zadorozhny, V. V. Uzhinsky, and S. Y. Shmakov, Yad. Fiz. **39**, 1165 (1984); Sov. J. Nucl. Phys. **39**, 729 (1984).
[28] C. Merino, I. S. Novikov, and Yu. Shabelski, Phys. Rev. C **80**, 064616 (2009).
[29] N. Metropolis, A. W. Rosenbluth, M. N. Rosenbluth, A. H. Teller, and E. Teller, J. Chem. Phys. **21**, 1087 (1953).
[30] G. D. Alkhazov and A. A. Lobodenko, Yad. Fiz. **70**, 98 (2007) [Phys. At. Nucl. **70**, 93 (2007)].
[31] S. Yu. Shmakov, V. V. Uzhinskii, and Zadorozhny, Comput. Phys. Commun. **54**, 125 (1989).
[32] D. Krpic and Yu. M. Shabelski, Z. Phys. C **48**, 483 (1990).
[33] B. Abu-Ibrahim and Y. Suzuki, Nucl. Phys. A **728**, 118 (2003).
[34] K. Varga, S. C. Pieper, Y. Suzuki, and R. B. Wiringa, Phys. Rev. C **66**, 034611 (2002).
[35] D.Chauhan and Z. A. Khan, Phys. Rev. C **80**, 054601 (2009).
[36] J. F. Liu, Y. S. Zhang, C. Y. Yang, J. F. Shen, and B. A. Robson, Phys. Rev. C **54**, 2509 (1996).
[37] V. Franco and A. Tekou, Phys. Rev. C **37**, 1097 (1988).
[38] P. Shukla, Phys. Rev. C **67**, 054607 (2003).
[39] L. A. Londratyuk and V. B. Kopeliovich, JETP Lett. (USSR) **13**, 123 (1971).
[40] R. J. Glauber and G. Matthiae, Nucl. Phys. B **21**, 135 (1970).
[41] W. Czyz, L. Lesniak, and H. Wolek, Nucl. Phys. B **19**, 125 (1970).
[42] W. R. Gibbs and R. Arceo, Phys. Rev. C **72**, 065205 (2005).
[43] G. Fäldt and H. Pilkuhn, Phys. Lett. B **46**, 337 (1973); **40**, 613 (1972).
[44] S. K. Charagi and S. K. Gupta, Phys. Rev. C **41**, 1610 (1990); **46**, 1982 (1992).
[45] M. H. Cha, Phys. Rev. C **46**, 1026 (1992).
[46] S. K. Charagi, Phys. Rev. C **51**, 3521 (1995).
[47] M. A. Alvi, J. H. Madani, and A. M. Hakmi, Phys. Rev. C **75**, 064609 (2007).
[48] I. Ahmad, M. A. Abdulmomen, and M. S. Al-Enazi, Phys. Rev. C **65**, 054607 (2002).
[49] R. J. Glauber, in *Lectures in Theoretical Physics*, edited by W. E. Brittin and L. G. Dunham, Vol. 1 (Interscience Publishers Inc., New York, 1959), p. 315.
[50] S. J. Wallace, Ann. Phys (NY) **78**, 190 (1973); Phys. Rev. Lett. **27**, 622 (1971).
[51] D. R. Harrington, Phys. Rev. **184**, 1745 (1969).
[52] R. D. Amado, J.-P. Dedonder, and F. Lenz, Phys. Rev. C **21**, 647 (1980).
[53] A. G. Sitenko, Ukr. Fiz. Zh. **4**, 152 (1959) [Ukr. J. Phys. **53** (special issue), 142 (2008)].
[54] M. E. Brandan, H. Chehime, and K. W. McVoy, Phys. Rev. C **55**, 1353 (1997).
[55] J.-P. Dedonder, W. R. Gibbs, and M. Nuseirat, Phys. Rev. C **77**, 044003 (2008).
[56] SAID program available at http://gwdac.phys.gwu.edu; R. A. Arndt, I. I. Strakovsky, and R. L. Workman, Phys. Rev. C **62**, 034005 (2000).
[57] S. Wallace, in *Advances in Nuclear Physics*, edited by J. W. Negele and E. Vogt (Plenum, New York, 1981), Vol. 12, p. 135, Tables III and IV.
[58] W.-M. Yao *et al*., J. Phys. G. Nucl. Part. Phys. **33**, 1 (2006); Nakamura *et al*. (Particle Data Group), J. Phys. G., Nucl. Part Phys. **37**, 075021 (2010).
[59] F. Sammarruca and L. White, Phys. Rev. C **83**, 064602 (2011).
[60] T. Furumoto, Y. Sakuragi, and Y. Yamamoto, Phys. Rev. C **80**, 044614 (2009).
[61] C. A. Bertulani and C. De Conti, Phys. Rev. C **81**, 064603 (2010).
[62] W. P. Madigan *et al*. Phys. Rev. D **31**, 966 (1985).
[63] P. J. Mulders, A. T. Aerts, and J. J. de Swart, Phys. Rev. D **21**, 2653 (1980).
[64] V. Lapoux *et al*., Phys. Rev. C **66**, 034608 (2002).
[65] J. S. Al-Khalili *et al*. Phys. Lett. B **378**, 45 (1996).,
[66] Y.-W. Lui, H. L. Clark, and D. H. Youngblood, Phys. Rev. C **64**, 064308 (2001).
[67] F. Nuoffer *et al*. Nuovo Cimento A **111**, 971 (1998).
[68] D. T. Khoa, H. G. Bohlen, W. von Oertzen, G. Bartnitzky, A. Blazevic, F. Nuoffer, B. Gebauer, W. Mittig, and P. Roussel-Chomaz, Nucl. Phys. A **759**, 3 (2005); D. T. Khoa, W. von Oertzen, H. G. Bohlen, and F. Nuoffer, *ibid*. **674**, 387 (2000).
[69] B. Bonin *et al*., Nucl. Phys. A **445**, 381 (1985).
[70] M. Buenerd, A. Lounis, J. Chauvin, D. Lebrun, P. Martin, G. Duhamel, J. C. Gondrand, and P. De Saintignon, Nucl. Phys. A **424**, 313 (1984); M. Buenerd *et al*., Phys. Rev. C **26**, 1299 (1982).
[71] P. Roussel-Chomaz, N. Alamanos, F. Auger, J. Barrette, B. Berthier, B. Fernandez, L. Papineau, H. Doubre, and W. Mittig, Nucl. Phys. A **477**, 345 (1988).
[72] T. Wakasa *et al*., Phys. Lett. B **653**, 173 (2007).
[73] J. Y. Hostachy *et al*. Nucl. Phys. A **490**, 441 (1988).
[74] T. Ichihara *et al*., Nucl. Phys. A **569**, 287c (1994).
[75] G. D. Alkhazov *et al*., Nucl. Phys. A **280**, 365 (1977).
[76] A. Chaumeaux, G. Bruge, T. Bauer, R. Bertini, A. Boudard, H. Catz, P. Couvert, H. H. Duhm, J. M. Fontaine, D. Garreta, and L. C. Lugol, Nucl. Phys. A **267**, 413 (1976).

[77] J. Berger *et al.*, Nucl. Phys. A **338**, 421 (1980).
[78] L. Satta *et al.*, Phys. Lett. B **139**, 263 (1984).
[79] H. P. Morsch, W. Spang, and P. Decowski, Phys. Rev. C **67**, 064001 (2003).
[80] H. P. Morsch *et al.*, Z. Phys. A **350**, 167 (1994).
[81] W. Czyz and L. C. Maximon, Ann. Phys. (NY) **52**, 59 (1969); **60**, 484 (1970).
[82] S. Gartenhaus and C. Schwartz, Phys. Rev. **108**, 482 (1957).
[83] W. Bertozzi, J. Friar, J. Heisenberg, and J. W. Negele, Phys. Lett. B **41**, 408 (1972).
[84] C. R. Ottermann, G. Kobschall, K. Maurer, K. Rohrich, Ch. Schmitt, and V. H. Walther, Nucl. Phys. A **436**, 688 (1985).
[85] A. von Gunten, Ph.D. thesis, Technische Hochschule Darmstadt, 1982 (unpublished).
[86] H. Chandra and G. Sauer, Phys. Rev. C **13**, 245 (1976).
[87] W. R. Gibbs, *Computation in Modern Physics* (World Scientific, Singapore, 2006).
[88] A. Vitturi and F. Zardi, Phys. Rev. C **36**, 1404 (1987).
[89] C. A. Bertulani and P. G. Hansen, Phys. Rev. C **70**, 034609 (2004).
[90] C. A. Bertulani and A. Gade, Comput. Phys. Commun. **175**, 372 (2006).
[91] J. S. McCarthy, I. Sick, and R. R. Whitney, Phys. Rev. C **15**, 1396 (1977).
[92] I. Sick and J. S. McCarthy, Nucl. Phys. A **150**, 631 (1970).
[93] J. J. Ullo and H. Feshbach, Ann. Phys. (NY) **82**, 156 (1974).
[94] W. R. Gibbs and J.-P. Dedonder, Phys. Rev. C **46**, 1825 (1992).
[95] I. Sick, J. B. Bellicard, J. M. Cavedon, B. Frois, M. Huet, P. Leconte, P. X. Ho, and S. Platchkov, Phys. Lett. B **88**, 245 (1979).
[96] M. Y. M. Hassan and Z. Metawei, Acta Phys. Slovaca **52**, 23 (2002).
[97] I. Ahmad, J. Phys G **6**, 947 (1980).
[98] C. W. De Jager, H. De Vries, and C. De Vries, At. Data Nucl. Data Tables **14**, 479 (1974) (Table I, ^{208}Pb, 2pF).
[99] H. M. M. Mansour and Z. Metawei, Ukr. J. Phys. **53**, 1043 (2008).
[100] D. Chauhan and Z. A. Khan, Phys. Rev. C **75**, 054614 (2007).
[101] M. A. Hassanain, A. A. Ibraheem, and M. El-Azab Farid, Phys. Rev. C **77**, 034601 (2008).
[102] M. C. Mermaz, B. Bonin, M. Buenerd, and J. Y. Hostachy, Phys. Rev. C **34**, 1988 (1986).
[103] H. Lesniak and L. Lesniak, Nucl. Phys. B **25**, 525 (1971).
[104] C. Ciofi Degli Atti and R. Guardiola, Phys. Lett. B **36**, 287 (1971).
[105] V. Yu. Denisov and N. A. Pilipenko, Phys. Rev. C **81**, 025805 (2010).
[106] G. E. Brown, *Unified Theory of Nuclear Models and Forces* (North-Holland, Amsterdam, 1967).
[107] J. P. Svenne and R. S. Mackintosh, Phys. Rev. C **18**, 983 (1978).
[108] J. L. Friar and J. W. Negele, Nucl. Phys. A **240**, 301 (1975).
[109] K. Hagino, N. W. Lwin, and M. Yamagami, Phys. Rev. C **74**, 017310 (2006).
[110] W. J. Vermeer, M. T. Esat, J. A. Kuehner, R. H. Spear, A. M. Baxter, and S. Hinds, Phys. Lett. B **122**, 23 (1983).
[111] M. H. Cha and Y. J. Kim, J. Phys. G **17**, L95 (1991).
[112] L.-B. Wang *et al.*, Phys. Rev. Lett. **93**, 142501 (2004).
[113] M. Abramowitz and I. A. Stegun, eds., *Handbook of Mathematical Functions* (Dover, New York, 1965).
[114] R. A. Malfliet and J. A. Tjon, Nucl. Phys. A **127**, 161 (1969).